



UPPSALA  
UNIVERSITET

*Digital Comprehensive Summaries of Uppsala Dissertations  
from the Faculty of Science and Technology 120*

# Colour Correction of Underwater Images Using Spectral Data

JULIA ÅHLÉN



ACTA  
UNIVERSITATIS  
UPSALIENSIS  
UPPSALA  
2005

ISSN 1651-6214  
ISBN 91-554-6403-3  
urn:nbn:se:uu:diva-6138

Dissertation presented at Uppsala University to be publicly examined in Polhemsalen, Ångström Laboratory, Uppsala, Friday, December 16, 2005 at 09:15 for the degree of Doctor of Philosophy. The examination will be conducted in English.

**Abstract**

Åhlén, J. 2005. Colour Correction of Underwater Images Using Spectral Data. Acta Universitatis Upsaliensis. *Digital Comprehensive Summaries of Uppsala Dissertations from the Faculty of Science and Technology* 120. x+55 pp. Uppsala. ISBN 91-554-6403-3.

For marine sciences sometimes there is a need to perform underwater photography. Optical properties of light cause severe quality problems for underwater photography. Light of different energies is absorbed at highly different rates under water causing significant bluishness of the images. If the colour dependent attenuation under water can be properly estimated it should be possible to use computerised image processing to colour correct digital images using Beer's Law.

In this thesis we have developed such estimation and correction methods that have become progressively more complicated and more accurate giving successively better correction results. A process of estimation of downwelling attenuation coefficients from multi or hyper spectral data is a basis for automatic colour restoration of underwater taken images. The results indicate that for each diving site the unique and precise coefficients can be obtained.

All standard digital cameras have built in white balancing and colour enhancement functions designed to make the images as aesthetically pleasing as possible. These functions can in most cameras not be switched off and the algorithms used are proprietary and undocumented. However, these enhancement functions can be estimated. Applying their reverse creates un-enhanced images and we show that our algorithms for underwater colour correction works significantly better when applied to such images.

Finally, we have developed a method that uses point spectra from the spectrometer together with RGB colour images from a camera to generate pseudo-hyper-spectral images. Each of these can then be colour corrected. Finally, the images can be weighted together in the proportions needed to create new correct RGB images. This method is somewhat computationally demanding but gives very encouraging results.

The algorithms and applications presented in this thesis show that automatic colour correction of underwater images can increase the credibility of data taken underwater for marine scientific purposes.

*Keywords:* Colour, Correction, Attenuation, Coefficient, Underwater

*Julia Åhlén, Centre for Image Analysis, Lägerhyddsv. 3, Uppsala University, SE-75237 Uppsala, Sweden*

© Julia Åhlén 2005

ISSN 1651-6214

ISBN 91-554-6403-3

urn:nbn:se:uu:diva-6138 (<http://urn.kb.se/resolve?urn=urn:nbn:se:uu:diva-6138>)

*To my dear mother*

An old red clay pot  
Resting on the ocean floor -  
The image is blue!

## List of Papers

This thesis is based on the following papers, which are referred to in the text by their Roman numerals.

- I Åhlén, J., Bengtsson, E., Lindell, T. (2003) Color Correction of Underwater Images Based on Estimation of Diffuse Attenuation Coefficients. *In Proceedings of the PICS 2003: The PICS Conference, An International Technical Conference on The Science and System of Digital Photography, including the Fifth International Symposium on Multispectral Color Science*, pp.325-329, Rochester,USA, May 2003.
- II Åhlén, J., Sundgren, D. (2003) Bottom Reflectance Influence on a Color Correction Algorithm for Underwater Images. *In Proceedings of the 13th Scandinavian Conference on Image Analysis (SCIA)*, volume 2749 of *Lecture Notes in Computer Science* pp.922-926, Göteborg, Sweden, July 2003.
- III Åhlén, J., Sundgren, D. (2004) Improvement of a Color Correction Algorithm for Underwater Images Through Compensating for Digital Camera Behaviour. *In Proceedings of the Swedish Symposium on Image Analysis*, pp. 142-145, Uppsala, Sweden, March 2004.
- IV Åhlén, J., Sundgren, D., Bengtsson, E. (2005) Pre-Processing of Underwater Images Taken in Shallow Water for Color Reconstruction Purposes. *In Proceedings of the 7th IASTED International Conference on Signal and Image Processing*, On CD-ROM, Honolulu, Hawaii, USA, August 2005.
- V Åhlén, J., Sundgren, D., Lindell, T., Bengtsson, E. (2005) Dissolved Organic Matters Impact on Colour Reconstruction in Underwater Images. *In Proceedings of the 14th Scandinavian Conference on Image Analysis*, volume 3540 of *Lecture Notes in Computer Science* pp. 1148-1156, Joensuu, Finland, June 2005.

- VI Åhlén, J., Bengtsson, E. (2005) Evaluation of Underwater Spectral Data for Colour Correction Applications. *Submitted for publication.*
- VII Åhlén, J., Sundgren, D., Bengtsson, E. (2005) Application of Underwater Spectral Data for Colour Correction Purposes. *Submitted for publication.*

Reprints were made with permission from the publishers. The work of this thesis was financed by Knowledge Foundation.

## Related work

The author has also contributed to the following publications:

- I        Åhlén, J. (2002) Acquisition and Colour Correction of Underwater Multispectral and Hyperspectral Images. *Seventh International Conference on Remote Sensing for Marine and Coastal Environments*, Miami, Florida, May 2002.
- II        Zdravkovic, J., Åhlén, J. (2004) Modeling Image Processing Tasks As Flexible Workflows for Improved Quality of Service. *The IADIS Applied Computing*, On CD-ROM, Lisbon, Portugal, March 2004.
- III       Åhlén, J., Bengtsson, E. (2004) On Colour Reconstruction of Underwater Images Taken in Shallow Waters. *In Proceedings of the Ocean Optics XVII*, On CD-ROM, Fremantle, Australia, October 2004.





# Contents

1	Introduction and Objectives	1
1.1	Goal and focus	2
1.2	About this thesis	3
2	Background	5
2.1	Light field	5
2.2	Optical properties of water	6
2.2.1	Inherent vs apparent optical properties	6
2.2.2	Diffuse attenuation coefficient	7
2.2.3	Dissolved organic matters and suspended inorganic matters	8
2.3	Underwater data collection	9
2.3.1	Spectralon	10
3	Colour image processing for underwater applications	11
3.1	Colour perception	11
3.2	R, G and B in digital cameras	12
3.3	Camera's enhancement functions	13
3.4	Colour correction	14
3.4.1	Underwater image restoration	15
3.5	Implementation	17
4	New methods and applications	19
4.1	Paper I, II	
	Estimation of diffuse attenuation coefficients for three spectral channels in a digital camera	19
4.1.1	Methods and experiments	20
4.1.2	Results	26
4.1.3	Conclusions	27
4.2	Paper III, IV	
	Estimation of camera enhancement functions and preprocessing of images	28
4.2.1	Methods and experiments	28
4.2.2	Results	32
4.2.3	Conclusions	33
4.3	Paper V	
	Dissolved particles influence on $K_d$ values	34
4.3.1	Methods and experiments	35

4.3.2	Results .....	36
4.3.3	Conclusions.....	38
4.4	Paper VI, VII	
	Spectral data applied on colour underwater image correction ..	39
4.4.1	Methods and experiments .....	39
4.4.2	Results .....	41
4.4.3	Conclusions.....	42
4.4.4	Results .....	44
4.4.5	Conclusions.....	45
5	Discussion .....	47
	References .....	53

# 1. Introduction and Objectives

The oceans cover more than 70% of the earth and yet their environment are the least explored by humans. Understanding the processes beneath the sea is of great importance for the health of our planet [2]. Coral reefs are damaged or dying in most of their natural habitats. Preserving them is beneficial for the economy and for the supply of food for millions of people. Alternative ways of monitoring coral reefs are the main application in the methods described in this thesis.

There are numerous ways to study the underwater world. A possibility to cover large geographic areas is given by remote sensing from satellites such as Landsat and aerial photography. Both these techniques provide estimates of coral health if underwater features can be properly identified. There are advantages and disadvantages with both these techniques. It is possible to study water properties but with the expense of low spatial resolution in case of Landsat data. Hyperspectral satellite-borne sensors offers high spectral resolution at potentially lower cost than higher spectral resolution airborne sensors. However, for small scale projects, the most economical systems are off the shelf cameras. In situ measurements are sometimes used as a complementary technique for remote and airborne sensing and can provide an important information about the water column, which gives a basis for quality analysis. In situ measurements require usage of camera systems when discrimination of small featured benthic habitats are needed. There are numerous methods for extracting values for water quality from spectral data measured under the water surface. These values can be used to estimate e.g. the chlorophyll or yellow substance concentrations of these waters, the latter often referred to as dissolved organic matters. Water column properties are affected by the amount of dissolved organic matters and suspended particles, which are always present.

Light, that penetrates the water body, is attenuated at a rate that depends mostly on the concentration of small particles and due to the absorption properties, light at longer wavelengths disappears first. Particles, which are smaller than a particular wavelength, will cause a regular Rayleigh scattering and larger particles will dictate in what manner light is reflected, transmitted and absorbed in a more irregular way.

In this thesis methods for computer aided colour correction of underwater images are presented. We need to examine how far light travels trough

the water and then apply this knowledge to our colour correction algorithm. The fundamental idea is to estimate the attenuation coefficients for the three wavelength bands of a standard camera, red, green and blue, at a particular diving site and then apply Beer's Law to correct the images. The camera itself together with a reflectance standard of known reflectance can be used to estimate the coefficients. This works well for some images. However, if the bottom reflectance is very high or very low, light reflected from the bottom will have a significant impact that need to be taken into account. When that factor is added to the correction model the fraction of the images that can be corrected in a satisfactory way increases.

A simplified approach to extract diffuse attenuation coefficients from the underwater images would give an easy way for scientists to study the colour information from different corals or bottoms at a resolution that is superior to satellite or airborne imagery.

A method for generating pseudo hyperspectral images from common three channel imagery and using this data for colour correction is presented. The proposed methods should make it possible to monitor coral reefs at a higher resolution than offered by remote sensing in a simple and economical way.

## 1.1 Goal and focus

The aim of this research is to develop new algorithms and techniques as well as improved methods giving marine scientists a fast and economically defendable way to collect and colour correct underwater images. For this project only data from shallow waters, where visible light are still present is considered. Corals are commonly found in such tropical waters. Before testing a colour correction algorithm on images there is a need to examine the digital camera built in functions. The effects, which in many cases will beautify the images will cause changes in data, making colour correction impossible. The papers included here will illustrate the collection, processing and restoration of underwater photography.

The focus has been on finding simple and potentially automated processes for colour correcting underwater imagery. Scientific efficiency can increase dramatically if divers will be able to rely on the data taken on a first try disregarding the poor quality of the images. Here we are mainly concerned with bluishness in images caused by the severe absorption properties of water.

There are well established methods to derive the necessary parameters to describe the optical characteristics of water column. However, there is as yet no focus on methods for colour correction of underwater images based on these characteristics. Our main purpose is to create the effect of water being removed from the photographed environment, meaning that we need to

study carefully what happens with light at a particular wavelength at different depths.

To be able to estimate the remaining light at an object and the diffuse attenuation coefficients under the water surface the measured intensity is analysed. We will distinguish between two approaches as to how these parameters can be estimated. One is from underwater images taken at decreasing depths with a reflectance gray plate present in each image and another is from point wise taken spectral data from decreasing depths. These approaches differ in the amount of values that can be obtained, which is equal to the amount of spectral channels of the measuring device.

Another discussion which we will bring up in the included papers is on the digital camera's enhancement functions, which for the most cameras are not possible to switch off completely. We will show how these functions can be estimated and removed from the resulting image as if they were switched off.

As a third viewpoint on colour correction we will consider the transformation from three channel images to pseudo hyperspectral data. The more spectral channels present in an image, the more accurate the colour correction. Here we aim to find a method for estimation of hyperspectral imagery without having to measure with expensive instruments.

## 1.2 About this thesis

Chapter two contains overviews of the light field, how it behaves when entering water. Techniques for estimating diffuse attenuation coefficients and methods for making measurements under the water are discussed. These are only short descriptions, but hopefully they contain enough information to familiarise the reader with the concepts used throughout the thesis.

Chapter three brings up the different steps of recording data on a CCD chip and digital image processing in general. The reader will be introduced to basic colorimetry concepts. The main emphasis is on light that can be captured and processed by digital cameras.

The material presented in chapter four is a description and discussion of the papers included in the thesis.

Chapter five concludes with a summary of the thesis, the results are discussed, and some future research areas are suggested.



## 2. Background

### 2.1 Light field

Light is envisioned as consisting of numerous localised packets of electromagnetic energy, called photons, which move through empty space with speed  $c = 2.998 \times 10^8 \text{ m s}^{-1}$ . The photon viewpoint of light is well suited to the development of radiative transfer theory, but the electromagnetic-field viewpoint on photons is convenient for certain types of problems, such as the scattering of light under the water surface.

The photons generated by the sun stream into space in all directions away from the sun. By the principle of conservation of energy, the total energy per time unit crossing an imaginary spherical surface of radius  $R$  measured from the sun's centre is independent of  $R$ . However, since the area  $4\pi R^2$  of the spherical surface increases as  $R^2$ , the energy per time unit per area unit of the sphere, which is called the irradiance, must decrease proportionally to  $R^{-2}$ . This result is known as the inverse square law for irradiance. At the mean distance of the earth from the sun, the solar irradiance from photons of all wavelengths,  $E_s$ , is near  $E_s = 1367 \text{ W m}^{-2}$ .  $E_s$  [3] is commonly called the solar constant. The photons arriving at earth from the sun are not all equally energetic. The energy of a photon is inversely proportional to its wavelength. Furthermore, the number of photons per wavelength interval is not uniform over the electromagnetic spectrum.

For measured spectral, or wavelength, distribution of the solar irradiance,  $E_s(\lambda)$ , over the wavelength band it is seldom necessary for optical oceanographers to concern themselves with the detailed wavelength dependence of  $E_s(\lambda)$ . It is sufficient to deal with  $E_s(\lambda)$  values averaged over bandwidths of order  $\Delta\lambda = 10 \text{ nm}$ , which correspond to the bandwidths of the optical instruments routinely used in underwater measurements. Moreover, it is not the solar irradiance at the top of the atmosphere, but the sunlight that actually reaches the sea surface, that is relevant to marine optics. The magnitude and spectral dependence of the solar radiation reaching the earth's surface are highly variable functions of the solar angle from the zenith (i.e. of the time of day, season and latitude) and of atmospheric conditions. In fact, the amount of light that reaches objects under the water depends strongly on the solar angle [6]. Irradiance  $E$  refers to photons incident onto a surface, where light that reaches the object under the water comes from the whole upper hemisphere

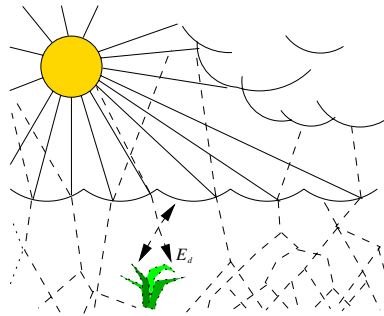


Figure 2.1: Illustration of light field under the water surface.

and is referred to as downwelling irradiance  $E_d$ , see Figure 2.1.

## 2.2 Optical properties of water

Natural waters, both fresh and saline, are mixtures of dissolved and suspended matter. These solutes and particles are both optically significant and highly variable in kind and concentration. Consequently, the optical properties of natural waters show large temporal and spatial variations and seldom resemble those of pure water. It is the connections between the optical properties and the biological, chemical and geological constituents of natural water and the physical environment that define the critical role of optics in aquatic research [26].

### 2.2.1 Inherent vs apparent optical properties

Inherent optical properties (IOP's) are those properties that depend only upon the medium. The two fundamental IOP's usually employed in ocean optics are the absorption coefficient and the volume scattering function, which are respectively the spectral absorbance and scattering per unit distance in the medium. For example, the total absorption coefficient  $a$  is the sum of absorption by the water itself, by various biological particles, by dissolved substances, by mineral particles, and so on. Since the composition of natural water bodies varies with location and time, so do the IOP's.

Apparent optical properties (AOP's) are those properties that depend both on the medium (the IOP's) and on the geometric structure of the ambient light field, and that display enough regular features and stability to be useful descriptors of the water body. Commonly used AOP's are the irradiance reflectance, the average cosines, and the various diffuse attenuation coefficients. These properties can be measured by radiometers or can be estimated from



spectral data. There are ongoing research studies on monitoring water optical properties. Accurate values can be obtained from mooring stations placed in a few off shore waters around the world [39].

### 2.2.2 Diffuse attenuation coefficient

Under typical oceanic conditions, for which the incident lighting is provided by the sun and sky, the various radiances and irradiances all decrease approximately exponentially with depth, at least when far enough below the surface and in shallow water to be free of boundary effects. It is therefore convenient to write the depth dependence of  $E_d(z, \lambda)$  as:

$$E_d(z, \lambda) = E_d(0, \lambda) \exp\left[-\int_0^z K_d(z', \lambda) dz'\right], \quad (2.1)$$

where  $K_d(z, \lambda)$  is the spectral diffuse attenuation coefficient for spectral downwelling plane irradiance. Solving for  $K_d(z, \lambda)$  gives:

$$K_d(z, \lambda) = -\frac{\partial \ln E_d(z, \lambda)}{\partial z} = -\frac{1}{E_d(z, \lambda)} \frac{\partial E_d(z, \lambda)}{\partial z}. \quad (2.2)$$

If we define  $\bar{K}_d(z, \lambda)$  as the average of  $K_d(z, \lambda)$  over the depth interval from 0 to  $z$ ,

$$\bar{K}_d(z, \lambda) \equiv \frac{1}{z} \int_0^z K_d(z', \lambda) dz', \quad (2.3)$$

then we can write Equation 2.1 as:

$$E_d(z, \lambda) = E_d(0, \lambda) \exp[-\bar{K}_d(z, \lambda)z]. \quad (2.4)$$

The difference between beam and diffuse attenuation coefficients is important. The beam attenuation coefficient  $c(\lambda)$  is defined in terms of the radiant power lost from a single, narrow, collimated beam of photons. The downwelling diffuse attenuation coefficient  $K_d(z, \lambda)$  is defined in terms of the decrease with depth of the ambient downwelling irradiance  $E_d(z, \lambda)$ , which comprises photons heading in all downward directions.  $K_d(z, \lambda)$  clearly depends on the directional structure of the ambient light field, hence its classification as an apparent optical property. In this thesis we are confined to diffuse attenuation coefficients, since we base the image restoration on estimated  $K_d(z, \lambda)$ :s, as discussed in section 4.1. We need to point out the obtained values universal usefulness listed in [33]:

- The  $K_d$  values are defined as ratios and therefore do not require absolute radiometric measurements.
- The  $K_d$ :s are strongly correlated with phytoplankton chlorophyll concentration, thus they provide a connection between biology and optics.

- About 90% of the diffusely reflected light from a water body comes from a surface layer of water of depth  $\frac{1}{K_d}$  thus  $K_d$ 's has implications for remote sensing.
- Radiative transfer theory provides several useful relations between the  $K_d$ s and other quantities of interest, such as the absorption and beam attenuation coefficients and other AOP's.
- Instruments are commercially available for the routine determination of the  $K_d$ 's.

We can calculate  $K_d$  values from estimated downwelling irradiances for each depth interval using Beer's Law, which is illustrated in Figure 2.2.

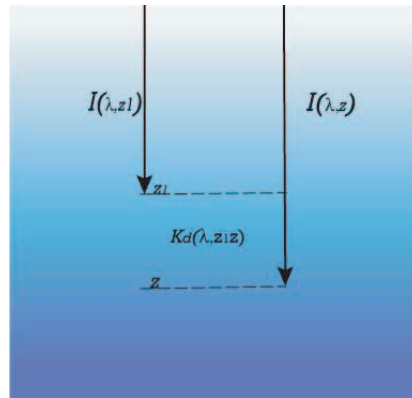


Figure 2.2: Illustration of Beer's Law.

### 2.2.3 Dissolved organic matters and suspended inorganic matters

Natural waters contain a large distribution of particles ranging from water molecules of size  $\sim 0.1$  nm, to small organic molecules of size  $\sim 1$  nm, to large organic molecules of size  $\sim 10$  nm, to viruses of size  $\sim 100$  nm and so on. Thus, water is composed entirely of particles. However, the constituents of natural waters are traditionally divided into dissolved and particulate matter, of organic and inorganic origins. When filtering a water sample, everything that passes through a filter whose size is roughly  $0.4\mu\text{m}$  is called dissolved matter, and everything retained on the filter is called a particle. Note that  $0.4\mu\text{m} = 400$  nm, the shortest wavelength of visible light. Thus optical microscopy is unable to resolve individual particles smaller than the dividing line between dissolved and particulate matter [26].

Concentrations of chlorophyll can be converted to absorption or attenuation coefficients, which are possible to derive from e.g. remote sensing reflectance using two or three spectral bands. Such studies has been performed by [23]. However, the method has not been tested on field data taken under the water by digital camera. Dissolved organic matters sometimes are referred to as yellow matters or CDOM and their absorbtion coefficients are possible to calculate from  $K_d$  values. The process is discussed in Paper V.

## 2.3 Underwater data collection

Taking pictures under the water is all about light and how it interacts with the small particles that water consists of. Underwater photographers usually set up a pair of strobes on the camera as an extra light source. The drawbacks are that the photographed object may be too large for conventionally mounted strobes, or the photographer working with strobes at depth may be unable to approach the object close enough to accommodate the limited illumination range of strobe lights [20]. In either case, the result is that the object is illuminated solely by ambient light in which red and yellow wavelengths may be deficient or totally absent when deep enough.

All the images and data used in the work leading to this thesis were acquired in shallow waters off the coast of Florida (USA), outside of Lisbon (Portugal) and off the Swedish east coast at the bay of Gävle. The authors of the papers were involved in the image acquisition in all cases. Since most of the images were taken under the water the authors were limited in the possibility to adjust the image acquisition. Most underwater imagery is of poor quality, which does not conflict with the authors goals. Data collected under the water usually ends up corrupted. The main focus of the work has, however, not been to produce high quality images, but rather images with enough quality for analysis and processing.

It is necessary to obtain spectral data for calculations described in Papers III, IV, V, VI and VII. In order to collect spectral data we set up the instrument as in Figure 2.3 and handed the end of the fiber cable (3) to the diver, which pointed it to the Spectralon (4) at different depths and the spectra were stored in the laptop. The process of setting up the equipment is as follows:

- Connect the Ocean Optics spectrometer to the laptop (1).
- Open Ocean Optics software.
- Using Ocean Optics spectrometer we take measurements of the light from the sky to get the light that is reflected on the surface of the ocean. To get these measurements, we aim the fibre optic to the sky.
- A diver will have to acquire the underwater data. A Spectralon [21] plaque is used to get the downwelling irradiance. The Spectralon plaque should be

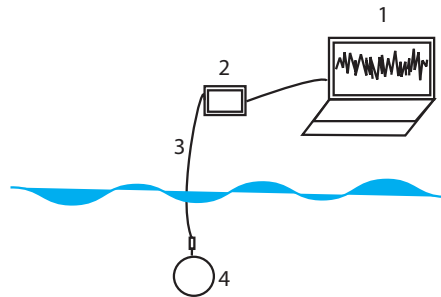


Figure 2.3: Pre installation of the instruments for underwater hyper spectral data collection.

levelled horizontally and the fibre optic should be aimed to the Spectralon plaque.

The angles should be respected, a zenith angle of  $45^\circ$  from the nadir direction.

- A dark measurement is done by blocking all incident light and store the result. Then press on spectrum and the scope mode minus dark. After we have subtracted the dark, the spectrum should be absolutely flat.

### 2.3.1 Spectralon

To obtain diffuse attenuation coefficients we needed to introduce some reflectance plate into the imagery. Such a gray plate called Spectralon is used in this study. There are two different types of Spectralon involved in the work leading to this thesis: diffuse white standard and a diffuse gray standard. Each standard is supplied with complete diffuse reflectance data from 250 - 2500 nm, every 50 nm. Spectralon diffuse white standards offer the highest diffuse reflectance values of any known substance.

The white standard present in the images in Papers IV to VII is durable, chemically inert with reflectance values of 99% and is spectrally flat over the UV-VIS-NIR spectrum meaning that it will reflect 99% of the incoming light. All Spectralon materials are typically flat to  $\pm 4\%$  over the range of 250 - 2500 nm and  $\pm 1\%$  over the photopic region of the spectrum. Spectralon reflectance standards and materials are highly lambertian over their effective spectral range.

### 3. Colour image processing for underwater applications

In this chapter the relation between the image acquisition and the resulting imagery will be introduced. Processing of images and further reconstruction of colours are the aims for this Thesis and therefore a proper introduction to digital imaging system and image reconstruction in general is needed. The restoration process of colours in digital images is highlighted in Section 3.4.

The described steps will be discussed in this chapter, and focus will be on the methods used in the research leading to this thesis.

#### 3.1 Colour perception

Our visual system selectively senses the range of light wavelengths that we refer to as the visual spectrum. Selective sensing of different light wavelengths allows the visual system to create the perception of colour. Colour receptors of the normal human eye (the cones) come in three distinct types, each of which is sensitive to only a part of the visible spectrum, see Figure 3.1.

For trichromatic matches to form a proper basis for a system of colour measurements, various parts of the experimental system must be specified. Many colour stimuli can be matched in colour completely by additive mixtures of three fixed primary stimuli whose radiant powers have been suitably adjusted [16]. In normal light the red, green, blue cone's spectral responses are:

- Blue: 400-540 nm, peak 440 nm, 2% absorbed.

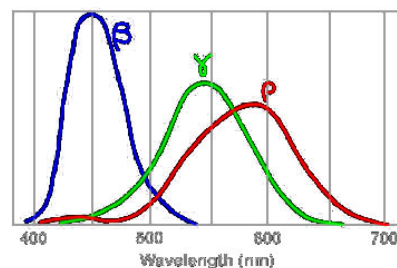


Figure 3.1: The sensitivity curves of the Rho, Gamma and Beta sensors in human eyes.

- Green: 400-640 nm, peak 540 nm, 20% absorbed.
- Red: 420-700 nm, peak 580 nm, 19% absorbed.

In situations with strong light, the retina produces three signals: R, G, B. These are processed to produce three outputs:

- Achromatic:  $R + G$ .
- Green: Blue-Yellow:  $(R + G) - B$ .
- Red: Red-Green:  $(R + B) - G$ .

This is why people are not able to see bluish yellow or reddish green, but can see reddish blue (magenta), greenish blue (cyan) etc.

### 3.2 R, G and B in digital cameras

A CCD chip is a monochrome light sensing device consisting of a discrete array of photosites, which can sense changes in brightness. CCD:s have a spectral sensitivity which is more heavily weighted towards infrared than it is towards blue, but nonetheless a CCD by itself can not discriminate colour. Colour information is obtained by putting coloured filters between the CCD and the subject [15]. The filtration can be on a per-chip basis, as is done in 3-chip cameras, or on a per-pixel basis, in 1-chip cameras.

Three-chip cameras also capture all three colours from each spatial location. Single-chip cameras employ one of three filter schemes: Bayer, see Figure 3.2, Complementary colour, see Figure 3.3 or hybrid Complementary-Primary design. All make use of a  $2 \times 2$  CCD element cluster to obtain luminance and chrominance information.

There is also a technology that allows full resolution images to be captured by a single chip. The image sensor employs three layers of photo detectors embedded in silicon. The layers take advantage of the fact that silicon absorbs different wavelengths of light at different rates, so the top layer records blue, the middle layer records green, and the bottom layer records red. This means that for every pixel location, there is a stack of three photo detectors. Such sensors are, however are not yet widely used.

The digital camera used for image acquisition in all the Papers leading to this thesis features complementary colour CMY+G pattern. The dye layers used for the cyan, magenta, and yellow filters pass more of the light to be filtered while blocking more of the light to be excluded. As a result chips using CMY+G filters tend to be almost twice as sensitive as chips using RGB filters.

A wide variety of colours can be obtained by mixing red, green and blue light in different proportions. A colour image is formed by making three measurements of scene brightness at each pixel, using the red, green and blue components of the detected light. The authors converted the CMY+G sensi-

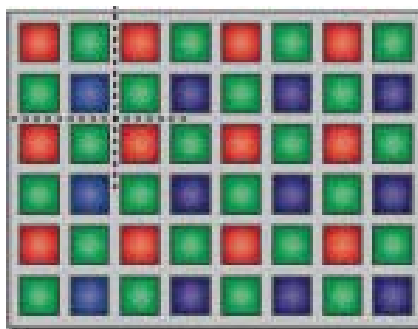


Figure 3.2: R G B Bayer pattern.

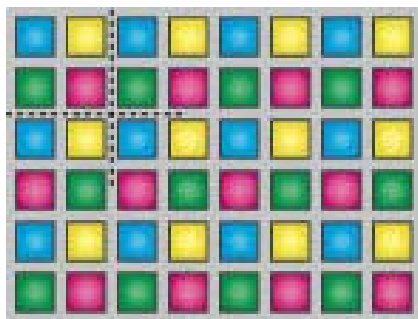


Figure 3.3: CMY and G complementary pattern.

tivity responses of the camera used in this study to the R G and B relative sensitivity curves, see Figure 3.4.

### 3.3 Camera's enhancement functions

All digital cameras have various in-camera image enhancement features, such as automatic noise reduction, in-camera image sharpening, contrast enhancement, etc. When doing image processing, the best results are obtained from using certain techniques on unprocessed images. Noise reduction can be performed later using software, where one presumably have more control over applying the algorithms than if letting the camera do it automatically [32]. Furthermore with a raw image it is possible to undo a processing action, or revert to the original raw image, if the results are not satisfactory. But anything that is done to the image in-camera before the data is saved cannot be undone.

Digital cameras have multiple white balance settings and usually provide both an automatic and a manual mode. If left in automatic mode, should the camera happen to select a different white balance setting for different expo-

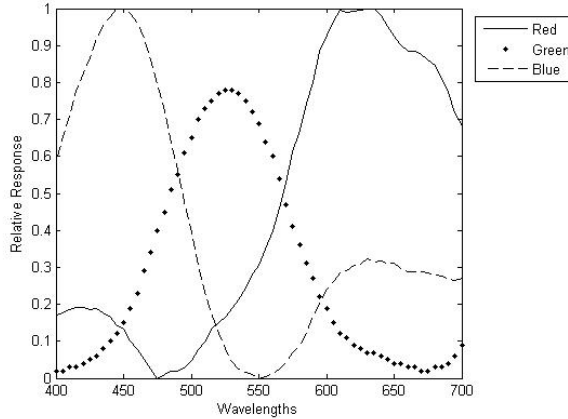


Figure 3.4: The relative sensitivity response for the red, green and blue spectral channels in the digital camera used for data acquisition.

asures of the same target, using those images for frame subtraction or image stacking/averaging will not produce the best results. In general, everyday photography one may not need accurate colour. We all want good colours in the digital images from our vacations, but accurate colour is important to people photographing for scientific use [11]. It is not always necessary for an image to be beautiful; but sometimes it has to be accurate and precise.

The enhancement functions can usually not be switched off completely. Even though it is possible to calibrate the RAW camera mode for light conditions that are expected during the shooting session, it is very hard to predict the changes in light under the water surface. In Papers III and IV the authors will discuss the estimation of those enhancement functions and remove the effects of them from the image.

### 3.4 Colour correction

When colour correcting underwater images the main focus is usually on balancing colours where blue colour can be prevailing [9]. Underwater photographers which are concerned with more natural colour representation in the images use filters, but filters cannot fix colour problems when shooting in ambient light at depths where red and yellow wavelengths of light are almost totally attenuated. Therefore a subjective approach to colour correction of underwater images is commonly used [7]. Image restoration aims at recovering the original image  $f(x,y)$  from the observed image  $g(x,y)$  using (if available) explicit knowledge about the degradation function  $h(x,y)$  and the noise characteristics  $n(x,y)$ . Restoration has an objective nature in contrary to the en-





Figure 3.5: a) Original image. b) Degraded with motion blur. c) Restored by Wiener filter

hancement of an image where all changes are made subjectively. An image can be colour corrected using filters on R, G and B vector space [34], where the outcome is subjectively defined in advance. Images are filtered depending on application both in the spatial and in the Fourier domain [35].

Most image restoration methods are based on convolution applied globally to the whole image. Those methods are referred to as deterministic and they are applicable to images with little noise and a known degradation function. In stochastic techniques the best restoration is sought according to some stochastic criterion, e.g., a least squares method and in some cases the degradation transformation must be estimated first. It is advantageous to know the degradation function explicitly. The better this knowledge is, the better are the results of the restoration. In most practical cases, there is insufficient knowledge about the degradation, and it must be estimated and modelled.

Wiener deconvolution can be used effectively when the frequency characteristics of the image and additive noise are known, to at least some degree [37]. In the absence of noise, the Wiener filter reduces to the ideal inverse filter as in Equation 3.1.

$$F(u, v) = \frac{G(u, v)}{H(u, v)}, \quad (3.1)$$

where  $F$  is the FFT of the image  $f$ ,  $H$  is the FFT of the distorting function  $h$  and  $G$  is the FFT of the observed image  $g$ . Application of the Wiener filter on a damaged image is illustrated in Figure 3.5

In order to calculate the degradation function a posteriori, knowledge must be obtained by analysing the degraded image. A typical example is to find some interest points in the image (e.g. corners, straight lines) and guess how they looked before degradation. Another possibility is to use spectral characteristics of the regions in the image that are relatively homogeneous [25].

### 3.4.1 Underwater image restoration

In underwater images blue tones are dominant due to the optical properties of water. Most of colour balancing methods are based on subjective user su-

Wavelength of absorbance maximum (nm)	Colour Absorbed	Colour Remaining
380-420	Violet	Green-yellow
420-440	Violet-blue	Yellow
440-470	Blue	Orange
470-500	Blue-green	Red
500-520	Green	Purple
520-550	Yellow-green	Violet
550-580	Yellow	Violet-blue
580-620	Orange	Blue
620-680	Red	Blue-green
680-780	Purple	Green

pervised approaches with aid of general purpose image processing software [5]. There are theoretical studies on how to connect spectral information from remotely sensed images to optical characteristics of water [23], however, no algorithms are developed to apply the obtained information to correct colours underwater images. It seems feasible that image processing should be possible to use to remove or at least significantly reduce the bluishness in the imagery. A number of works have addressed this issue. E.g the authors of [9] use a demosaicing technique in order to estimate the value of pixels that are unknown due to lack of light under the water. However this reconstruction method gives low saturated colours in the image, which makes it unsuitable for our application. The authors of [29] use regression models to correct colours, however to provide satisfactory results the described method requires a high number of observations. In the applications suggested in this thesis the divers are limited by the amount of time they can remain under water and thus can not take a large number of images.

When a substance absorbs light of a certain wavelength (colour), it depletes the transmitted light in precisely those wavelengths that are absorbed. For this reason, a solution that appears blue to the human eye does not absorb blue light. Rather, it is blue because it absorbed orange light, and allows all other wavelengths to pass unhindered (giving a bluish colour to the transmitted light, see Table 3.4.1 [17]). Light of longer wavelengths will be absorbed prior to shorter wavelengths. Blue light originates from relatively short wavelengths, which are of a higher energy and thus remains longer when descending under water.

The first step for any image processing is to prepare the instruments to acquire the imagery. For our underwater application we need to make pre

installations of the camera and sometimes also of the spectrometer prior to entering the water.

As a second step we pre-process the images to minimise the effects caused by built in enhancement functions. The effects of camera built in functions are discussed in Section 3.3. In the next step we should calculate or estimate some value that will be a basis for reliable colour restoration purposes. These values in our study are called diffuse attenuation coefficients and are briefly presented in Section 2.2.2. After inserting the obtained coefficients into the colour correction algorithm which will be given a discussion in section 4.1 we are able to restore colours to a certain extent.

For colour correction purposes we need to establish a degradation function so that it can be removed from the obtained imagery. The model of degradation is based on the rate of change of light with depth. We argue that those predictions can be made by analysing the diffuse attenuation coefficients from each diving site. The coefficients are derived from the images or spectral pointwise measurements taken at accurately registered depth. The methods for estimating these coefficients will be discussed in Papers I, II and V.

We are searching for methods to colour restore underwater imagery taken by inexpensive digital cameras. The more spectral channels that are available, the more accurate the colour correction would be. However, at present, hyperspectral imagery can only be acquired with expensive instruments and usually at the expense of low spatial resolution. There are studies that propose methods of transforming multispectral data into hyper spectral data using multiple filters [12]. For underwater imagery sessions it is highly unpractical to handle the filters that are currently available. Also, filters absorb light and lack of light is already a problem with underwater photography. In Paper VII the authors describe a simple and easy-to-implement model for transforming RGB images to a pseudo hyperspectral set of images. We only need to have at our disposal the relative sensitivity profile of the camera and spectral pointwise measurements of red, green and blue patches together with the RGB images.

### 3.5 Implementation

All proposed algorithms were implemented by the author or in cooperation with David Sundgren. The code is written in Matlab, which is well suited for image processing purposes. One drawback with Matlab is that of time efficiency. Images that were used for Papers I, II, III, IV, V and VI are  $1036 \times 2024$  pixels and colour restoration of such an image takes 5.6 seconds on a 1.9 GHz processor. For Paper VII where hyperspectral imagery is involved the calculation time is  $|L|/3$  times higher, where  $|L|$  is the number of spectral channels.



## 4. New methods and applications

### 4.1 Paper I, II

#### Estimation of diffuse attenuation coefficients for three spectral channels in a digital camera

By studying the living and non-living objects submerged in the seas, important information about global earth health can be derived [10]. We concentrate in this work on studying the underwater world by taking digital images. However, natural waters are not the friendliest environments for photographing purposes. Among remote sensing, aerial photography and water samples, underwater photography is a powerful tool for monitoring the changes in marine natural habitats [31]. Analysis of the photographed underwater environment provides a cheap and fast way to examine coral reefs in much higher resolution than other known methods.

To predict the outcome of the underwater imagery is a very difficult task if not impossible. It is therefore important to have methods to improve the image quality afterwards. Lightning conditions changes rapidly (e.g. due to clouds) and surface waters are moving randomly creating waves. This alters the incoming light, which makes calibration of the camera a challenging process. Pre-installations of the camera are usually done before entering the water, since the divers are limited in fine motor ability and time under the water. Impossibility to control cameras settings is yet another limitation for underwater photographers [20].

Since water absorbs lower energy wavelengths first, the colours disappear in the following order as we descend underwater: red, orange, yellow, green, blue and indigo. For underwater photography it means that even in shallow waters the images end up bluish. The loss of colour is based on the total distance the light travels, not just depth, due to the magnitude of the scattering, which is virtually independent of wavelength. The more water there is between the light source, object and the camera, the fewer colours will remain. This is a typical optical nature of ocean water, which will make images blue-coloured.

Paper I and II discuss whether anything can be done to remove or diminish the effects of light absorption in underwater imagery. The perception of colour depends not only on the spectral characteristics of the light source and the human eye, but especially on those of the object itself since all objects ab-

sorb, transmit and reflect incident radiation to varying degrees depending on their chemical/molecular composition and the wavelength of the energy. Open water and every object under the water surface also has a spectral signature, which represents the character of the electromagnetic energy reflected from that feature [14]. In natural waters, there is turbidity, which is a term used to describe the amount of particulate matter, and it is strongly correlated to the backscattered light. The higher the turbidity, the more light that is absorbed and scattered. This sort of predictable characteristic is what defines a spectral signature, and thus allows the quantification of a wide range of land cover types. In Paper I the authors show the relative reflectance of different bottom types derived from the imagery.

It is difficult to predict a priori the original colours of underwater objects; thus the restoration of colours of “bluish” underwater images is considered a difficult task. In Paper I and II colour disappearance with depth will be shown as a function of  $K_d$  against the depth. A digital camera in an underwater housing was used to produce underwater imagery. A neutral colour, highly lambertian reflecting plaque is used as a reference target and is present in each image.

It was noticed that extremely high or low values of the bottom reflectance have a negative effect on the algorithm. In Paper I the outcome of the algorithm was successful in 60% of the cases. Paper II introduces a bottom reflectance compensation function to the model presented in Paper I. We are focusing on shallow waters with various bottom types.

#### 4.1.1 Methods and experiments

The goal of Paper I is to estimate the diffuse attenuation coefficients  $K_d$  for three wavelengths in the red, green and blue electromagnetic intervals using only underwater imagery. These values are then set into Beer’s law and the light disappearance with depth can be predicted. Based on Beer’s Law a colour correction algorithm is created. In Paper II the effect of bottom reflection is taken into account and compensated for in the colour correction algorithm.

##### **Calculation of diffuse attenuation coefficients: Paper I**

In Paper I we show the effects of colour correction of underwater images by estimating the disappeared light and then adding it to the image. The authors argues that for each spectral channel red, green and blue the corresponding attenuation coefficient can be calculated. The coefficients  $K_d$  act as absolute values that determine the degradation for colour restoration purposes.

Paper I and II uses the well known equation Beer’s Law, which states that photons when entering an absorbing medium behaves according to Equation 4.1.



(a) Original image taken at 12 m of depth.



(b) Colour corrected by applying the  $K_d$ 's which have an effect of bringing up the image to 3 m of depth.

Figure 4.1: Underwater image colour corrected.

$$I = I_0 e^{-kz}, \quad (4.1)$$

where  $I$  is the observed intensity,  $I_0$  is the original light intensity,  $k$  is an absorption coefficient and  $z$  is the distance travelled through the medium. Below we will denote  $k$  by  $K_d$ . The absorption coefficient is traditionally expressed in units of  $1/\text{cm}$  (inverse cm) and  $z$  in cm [38]. Equation 4.1 holds for a single wavelength. At other wavelengths, the diffuse absorption coefficient is different, and the observed intensity varies. The absorption coefficient as a function of wavelength is a fundamental parameter describing the interaction of photons with a material. The result of colour correction based on Beer's Law and estimated  $K_d$  values is shown in Figure 4.1.

The process is initiated by estimation of relative reflectance, which is considered as the ratio of the intensity of reflected radiant energy to that reflected from a defined reference standard. Spectralon is chosen as such a reference standard. When collecting underwater imagery the reflectance standard is placed on a surface next to the target such as coral or other bottom type and imaged as part of the scene. Reflectance imagery is obtained by rationing the

three spectral channels of the scene divided by a mean pixel value of a gray reflectance panel measured at the same depth.

The relative reflectance corresponding to the same bottom type, but calculated from the different areas in the image will differ in amplitude, but nevertheless will have the same shape. Reflectances of randomly selected pair of bottom types such as brown algae are shown in Figure 4.2.

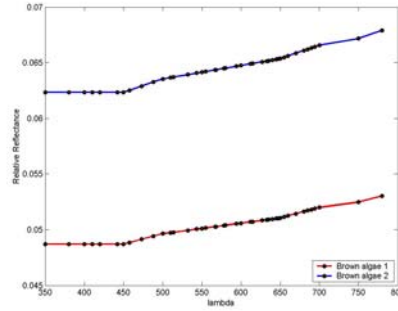


Figure 4.2: Reflectance of two brown algae areas in the same image

Estimation of the reflectances is done under the assumption that the Spectralon is taking in as much light as the surrounding environment in the image. Each pixel in each channel of the image can be assigned its own value of reflectance by using the Equation 4.2. We perform a spectral characterisation of the image acquisition system to establish the spectral model. Sensitivity curves of red, green and blue channels for the digital camera are studied, see Figure 3.4. The relative sensitivities of the wavelengths that are tabulated for the Spectralon are interpolated from the measured relative sensitivities.

$$R = \frac{I}{L_{in}} = \frac{I}{\frac{L_{out}}{R}} = \frac{IR}{L_{out}}, \quad (4.2)$$

where  $I$  is the radiation striking the lens, which is the intensity of the image,  $L_{in}$  is the radiation incident on the object (which is the same as on the Spectralon) and  $L_{out}$  is the intensity value of a Spectralon on the image. The above calculation is a simplification that does not take into account additional factors such as incident and reflection angles. However, it does enable the authors to calculate the relative reflectance at any point in the image in each channel.

As a next step we calculate the rate at which light of each wavelength will be absorbed by the water column. Since we are working with a digital camera, we are only able to estimate this rate for three appropriate wavelengths from each spectral channel: red, green and blue. The absorption of light will increase with depth and since we take images at a distance of 50 cm from each other we are able to introduce the depth parameter and calculate the absorption



coefficient as a function of wavelength and depth, see Equation 4.3.

$$K(z, \lambda) = -\frac{1}{L(z, \lambda)} \frac{\partial L}{\partial z}, \quad (4.3)$$

where  $z$  is the depth.

To estimate the incoming light at the surface for any particular wavelength we use the obtained reflectance values. We divide the mean intensity value of any object in the image by the estimated reflectance value of that object. In Paper I we rely on the reflectance value of the Spectralon. In fact, a series of vertical profiles of each channel provides relative  $E_d(z)$  to derive a  $K_d$  meter for three wavelengths.

As we have established the incoming light at the Spectralon and we assume that this gray plaque take in as much light as every object in the image, we can use Equation 4.3 to estimate the  $K_d$  values for an appropriate wavelength at each depth where an image was taken.

In the application the acquired images are used to predict changes in colour with changing depth.

As a next step we will insert  $K_d$ :s for Red, Green and Blue light into Equation 4.1 to estimate the loss of these particular colours in underwater images. When we apply this equation to our particular image at depths  $z$  and  $z_1$  meters it will be rewritten as in Equations 4.4 and 4.5.

$$I(z) = I_0 e^{-k(z)z}, \quad (4.4)$$

$$I(z_1) = I_0 e^{-k(z_1)z_1}. \quad (4.5)$$

In both calculations we are referring to  $I_0$ , which is the incoming light at the surface. This parameter will cancel out when we solve Equation 4.4 for  $I_0$  and insert  $I_0 = I(z) e^{k(z)z}$  into Equation 4.5. As we would like to visualise how much light is disappearing with depth we need to calculate the new intensity values for Red, Green and Blue channels in the image. In Equation 4.6 the new intensity values are calculated for the image taken at  $z$  m of depth. The result will be intensity values as if this image was taken at  $z_1$  meters depth.

$$I(z_1) = \frac{I_z}{e^{-K_d(z)z}} e^{-K_d(z_1)z_1}. \quad (4.6)$$

The new intensities are obtained for each spectral channel using downwelling attenuation coefficients  $K_d$ :s for each of these three channels.

Another issue is how background reflectance, in our case bottom reflectance, affects the process, and how this effect can be dealt with. This question is addressed in Paper II.

### **Estimation of bottom reflectance function, Paper II**

The objective of Paper II is to estimate and insert the bottom reflection function into the colour correction algorithm described in Paper I. A set of underwater images was tested by the algorithm and it was noticed that in 40% of the cases the outcome was erroneous. By examining the images where colour correction failed, we discovered that in most of these images extremely high or extremely low bottom reflection was observed and thus should be included as a significant variable. Bottom spectral reflectance quantifies the effect the optical characteristics of the bottom sediments have on the upwelling light field. In optically shallow waters which possess a large bottom component in the upwelling light field, light reflected from the bottom can be backscattered into the upward irradiance stream and influence the spectral content of the measured downwelling signal [8]. The extent to which this occurs is important to quantify because the measurement of object reflectance is biased by this process.

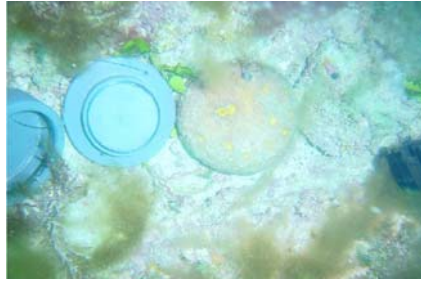
The presence of bottom reflected light could make colour correction for underwater environments easier because of the additional light, however extreme bottom reflectances has the effect of making the reflectance of objects in the image appear different from their actual values. In this Paper we suggest a method to compensate for this. An illustration of the performance of altered colour correction algorithm with built in bottom reflection function is shown in Figure 4.3.

The robustness of the algorithm was tested on images with both extremely high and low bottom reflectances as well as on images with normal bottom reflectances.

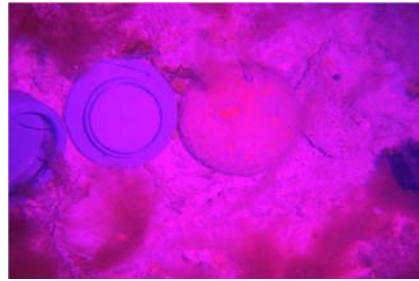
### **Estimation of bottom reflection function from the imagery**

The incoming light should decrease with depth according to Beer's law and the intensity of a pixel should be proportional to the incoming light. There are other parameters that can affect the strictly exponential disappearance of light with depth, the unknown camera white balancing functions is one them. We adress this issue in Section 4.2. However, in this particular imagery set we have assumed that camera behaviour affects the real outcome less than the bottom reflectance. To estimate the bottom reflection function we compare intensity profiles of pairs of images at the same depth but with different bottom types. The grey Spectralon reference target serves as a sample target and we observed high deviations in intensity profile from pair to pair. This suggests that images with intensity values from a Spectralon that are abnormally higher than a corresponding pair can be considered noisy due to bottom reflectance variations.

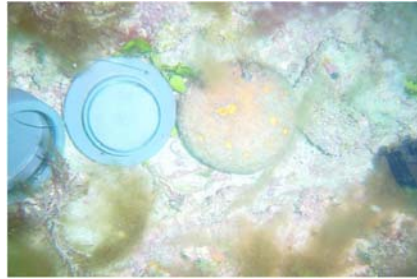
To develop a compensation function we need, as a first step, to calculate the incoming light at the surface and estimate the remaining light at the actual



(a) Original image taken at 15 m of depth.



(b) Colour corrected by applying the  $K_d$ :s which have an effect of bringing up the image to 3 m of depth.



(c) Colour corrected with bottom reflectance function built into Beer's Law.

Figure 4.3: Underwater image colour corrected by bringing it up to 1.6 m depth.

depth. This is possible since we already have  $K_d$  values for each depth and we also have a measurement of the Spectralon at the surface. By inverting Beer's Law we can predict the incoming light  $I_0$  at the surface.

The apparent reflectance of the Spectralon, which is based on intensity values from the images, as a function of bottom reflectance can be expressed as in Equation 4.7

$$R_{as} = R + f(R_{\text{bottom}}). \quad (4.7)$$

It should be pointed out that this equation holds for any object in an image since we assume that light is distributed equally on the whole image. This makes it possible to estimate the effect of bottom reflectance on any object given that the underwater environment is of the same type as in the reference image and at the same depth.

To produce the compensation function, the authors used a sequence of images with varying bottom reflectance from the same depth to obtain the apparent Spectralon reflectance. The reflectance of the Spectralon is based on an estimation of incoming light. Bottom reflectances were plotted against the

apparent reflectance of the Spectralon and the compensating function as displayed in Equation 4.8 is then obtained from these values.

$$f(R_{\text{bottom}}) = R_{\text{as}} - R. \quad (4.8)$$

To introduce the compensation function into Beer's Law, we replace  $I_z$  in Equation 4.6 with  $\frac{(R_r - f(R_{\text{bottom}}))L_{\text{out}}}{R}$ , where  $R_r$  is the reflectance of a typical object in the image,  $f(R_{\text{bottom}})$  is the function that describes how the bottom reflectance affects the apparent reflectance of the object,  $L_{\text{out}}$  is the pixel intensity value and  $R$  is the measured reflectance of the Spectralon. The resulting colour correction formula based on Beer's Law with bottom reflectance compensation function is in Equation 4.9

$$I(z_1) = \frac{(R_r - f(R_{\text{bottom}}))L_{\text{out}}}{R} e^{K_d(z)z - K_d(z_1)z_1}. \quad (4.9)$$

As can be seen the use of the colour correction algorithm with the compensation function inserted will work with the underlying assumption that light disappears at an exponential rate.

#### 4.1.2 Results

Applying the colour correction algorithm on an image that is corrupted due to water column optical properties results in an improvement in colours. Experimental results showed that for coral reef monitoring, in this particular area, we do not need to bring up the image to the surface since  $K_d$  for 3 meters depth and at the surface are not significantly different in these waters.

Due to noise, measuring error and bottom reflectance properties, the  $K_d$  values obtained by experimental data do not increase with depth strictly exponentially; the difference can be due to unknown camera behaviour with light changes.

As could be expected, the  $K_d$  curve for the Red channel is the most jagged since the lack of light makes Red the noisiest channel. When applying this algorithm to a corrupted image a significant improvement in colours could be observed. The effects of the water column that make images bluish are diminished.

In presence of extreme bottom reflectances the resulting  $K_d$  values produce erroneous results when used in the algorithm. The resulting images are heavy in magenta or blue. That is due to over or under estimated  $K_d$  values mostly for the red channel.

Using an improved model for colour correction of underwater images we are able to remove the negative effects of water column properties always present in underwater images almost irrespective of bottom reflectance. We

point out that bottom reflectance is not the only factor that could contribute to poor results of the algorithm. Such factors could be unpredictable behaviour of the CCD sensor, difficulties obtaining the exact depth and measurements of incoming light.

As we are using only a digital camera and a Spectralon our calculations are not exact. However this method is inexpensive yet reasonably accurate. After introducing the compensating function into the equation we could restore the colours in 80% of the tested images.

### 4.1.3 Conclusions

The spectral signature of bottom pairs such as brown algae in Figure 4.2 is identical. This agrees with the initial hypothesis for the project, that is, object reflectance in the underwater taken images would be adjusted by the Spectralons reflectance characteristics. However, if the assumption that the Spectralon takes in as much light as the environment in the image cannot be satisfied (i.e. the subject of investigation lies considerably deeper or shallower than the reflectance target) the relative reflectance is impossible to estimate. In this case we need to introduce a depth parameter for different objects in the image in the equation. However, that is not in the scope of the project.

In the image of an underwater scene the only dominant colour is blue. However, while diving we observe many colours including red. This phenomenon is explained by human vision having a highly adaptive spectral sensitivity. Cameras sensitivity follows linear light adaptivity, which will be shown in Paper IV.

To convert the camera output signals to device-independent data, several approaches were tested. Only one could be fully developed during this project. The method is based on the spectral model of the acquisition system and the gray reflectance target. By inverting the model, we can estimate the spectral reflectance of each pixel of the imaged surface.

For each diving site it is enough to estimate the  $K_d$  values only once and then use them for further processing of the images provided that the conditions are not changing. The weather changes and biological processes in the water can cause changes in optical water properties. In this case the  $K_d$  values will change and should be estimated again.

The assumption that light diminishes at an exponential rate with depth can be wrong in cases where dissolved organic matters and other substances are concentrated in layers. This issue is addressed in Paper V.

## 4.2 Paper III, IV

### Estimation of camera enhancement functions and preprocessing of images

While colour correcting underwater images, as described in section 4.1, we discovered that another parameter such as the camera enhancement function should be taken into consideration. The exact behaviour of those functions is kept as trade secrets and they are in most cameras not possible to shut off completely. Camera behaviour in unpredictable light conditions will be investigated in Paper III and IV. When planning, acquiring, configuring and operating an imaging system for use under water some issues concerning optical water properties should be discussed. According to the water column property and scattering of light in the sea it is difficult to predict the direction of light after it penetrates the surface; the loss of colour is based on the total distance it travels, not just depth [4]. Calibrating the camera for underwater photography is therefore a very challenging task.

The transmittance factor of the water mass between the camera and the object could be compared to the atmosphere and treated as described in [24]. However, the method requires much more precise measurements of the spectra and ground truth studies. We assume that the transmittance factor of water is the same for the whole imaged scene. The values of the pixels in a colour image correspond to the relative values of reflectance in different regions of the spectrum, normally in the red, green and blue regions. All digital cameras include some automatic white balancing and other image beautifying functions that change the relative sensitivities of the spectral channels depending on how much light of different colour composition did strike the chip [15].

The aim of Papers III and IV was to develop and test an easy to use method for removing the effects of the camera's own enhancement functions. We are presenting a method for estimation of correction coefficients, which are then used to preprocess the images taken with digital cameras with unknown behaviour. Further, we are showing that those functions are working uniformly and linearly over the whole image. Two digital cameras are tested and the results are illustrated. We make the reasonable assumption that the proposed method will generalise to other digital cameras.

#### 4.2.1 Methods and experiments

A field experiment was carried out to obtain imagery and spectral data of different underwater objects. Test imagery was collected off the coast of Lisbon in April 2004. Two different digital still cameras were used to take images of underwater objects at various depths, varying from 1.8 metres to 6.0 metres. Image format for one of the cameras is TIFF uncompressed with  $2048 \times 1536$

pixels. The other camera was set to take images at a size of  $1\,600 \times 2\,000$  pixels. A 99% reflectance [21] standard was photographed within the each scene. Together with the gray standard we placed a coloured plate in each photographed environment. The distance from the camera to the objects is approximately 45 cm.

The spectral data is obtained with a spectrometer [27], which pointwise measures the light intensity as a function of wavelength. The spectrometer, which will act as a calibration device, is placed over each coloured strip and over the reflectance plate and measures the intensity over the available 1 024 spectral channels. This data is then used to calculate the correction coefficients for the camera. The procedure was repeated at different depths. Since the spectrometer does not have built in enhancement functions and we do measurements very close to the object, the spectrometer's values can be assumed to be unaffected by transmittance and enhancement functions.

The amount of light recorded by the CCD chip is the light that is reflected from the objects and transmitted through water, see Equation 4.10.

$$I_{\text{ccd}} = E_d R_{\text{obj}} T, \quad (4.10)$$

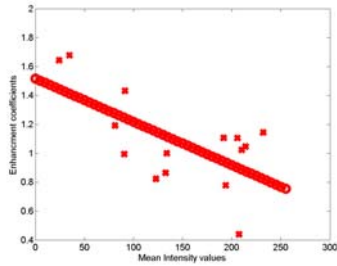
where  $E_d$  is the light incident on the object,  $R_{\text{obj}}$  is relative reflectance of the object and  $T$  is the transmittance factor of the water masses between the object and the camera.

#### **Estimation of camera enhancement function, Papers III and IV**

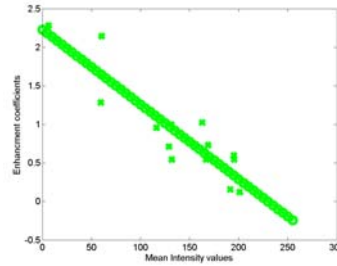
As the first step in the process of recovering an original image, which is unaltered by the built in function, we will consider the spectra from each coloured strip: red, green and blue. In Paper III we are taking pointwise data of coloured patches under the water in a swimming pool and making intensity counts with a spectrometer for each colour: red, green, blue and yellow. It should be pointed out that we do not need to collect the imagery under the water for the pre-processing step.

We calculate a ratio by considering a pixel with intensity in the top 95 percentile of red, green and blue, respectively, and spectrometer value in the top 95 percentile of red, green and blue measurements. By spectrometer measurements of red, green and blue we mean the total spectra when the instrument is placed above the red, green and blue plates, respectively. This ratio is referred to as an enhancement coefficient. In Paper III we assumed that the enhancement function in the camera, which modifies each registered colour value, is a function of the overall distribution of intensity values in the image. In Figure 4.4 we are showing that the functions are working not only uniformly but also linearly on the image.

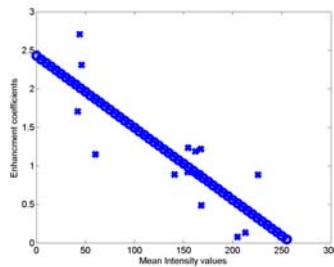
We multiply each pixel in the image by the coefficients obtained for the red,



(a) Plot of enhancement coefficients versus mean intensity values for red.



(b) Plot of enhancement coefficients versus mean intensity values for green.



(c) Plot of enhancement coefficients versus mean intensity values for blue.

Figure 4.4: Plot of enhancement coefficients versus mean intensity values for red, green and blue channels for images taken by digital camera 1.

green and blue channels, respectively. We call this a pre-processing step. The changes in colouring are aesthetically less appealing, however we can notice that there are close points of similarity between the pre-processed image and the reality that was observed by the eye, see Figure 4.5.

In Paper IV we are testing the described approach on a set of underwater images taken with two different digital cameras. An image will go through a pre-processing step where the intensity value is multiplied with the corresponding coefficient taken from the linear function. We can see an illustration of this procedure in Figure 4.6.

The pre-processed images are then put through the colour correction algorithm. This is done to be able to evaluate whether camera behaviour is crucial when considering colour restoration. Attenuation coefficients  $K_d$ 's are estimated according to the procedure described in section 4.1.1 to imitate water removal. By this we are “lifting up” the image to the surface with the help of Beer’s law. The method is found in Section 4.1. The pre-processed and colour corrected images are in Figure 4.7.

In Paper III we evaluate the camera behaviour significance by comparing



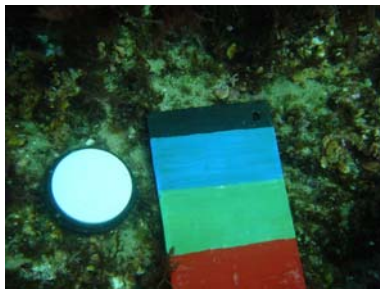


(a) Image taken under water with digital camera at 3.8 meters depth.

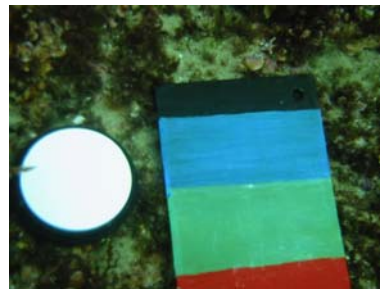


(b) Corrected with coefficients.

*Figure 4.5:* Image taken in the pool and then subjected to correction coefficients established by the method described here.



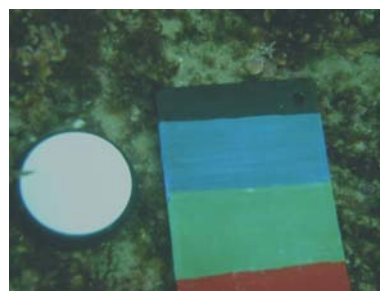
(a) Image taken by camera 1.



(b) Image taken by camera 2.

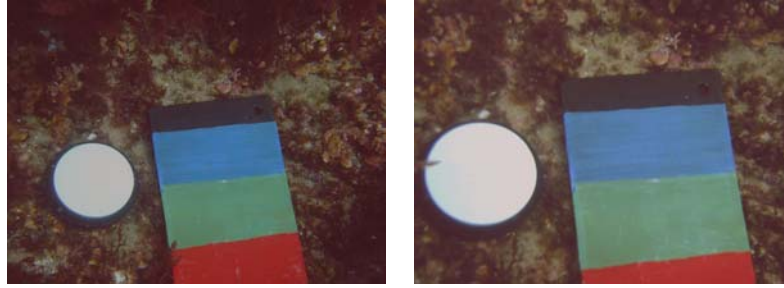


(c) Pre-processed image taken by camera 1.



(d) Pre-processed image taken by camera 2.

*Figure 4.6:* Underwater images taken with two digital cameras and subjected to pre-processing.



(a) pre-processed and colour corrected image taken by camera 1. (b) pre-processed and color corrected image taken by camera 2.

Figure 4.7: Images from Figure 4.6 (c,d) that have gone through colour correction.

the image pre-processed with the coefficients and colour corrected with the effect of removing the water with the image that was colour corrected without the pre-processing step. To evaluate the significance of pre-processing we compare the mean intensity values in red, green and blue spectral channels in the images that were corrected with and without pre-processing step.

#### 4.2.2 Results

By testing two different cameras we see a clear linear tendency of built in camera enhancement functions, see Figure 4.4. The deviations observed in the curves are most likely due to measurement error and the fact that we neglected the effect of water transmittance. We find that the colour correction algorithm performs better when applied to images that are preprocessed, see Table 4.1, by looking at the mean intensity values for the three spectral channels. Pre-processed image that was subjected for colour correction algorithm has the same mean intensity value for the red channel as the image that was taken on the surface.

	non pre-processed and colour corrected	non pre-processed surface image	pre-processed and colour corrected	pre-processed surface image
Red	142	225	107	107
Green	140	121	117	102
Blue	114	98	113	94

Table 4.1: Average intensity values of pre-processed respectively non pre-processed pairs of images that were colour corrected.

Pre-processing is accomplished by estimating correction coefficients using spectral reflectance data. The pre-processed images have considerably less red light than the unprocessed. This effect is due to the fact that the camera functions adjusts white balance so that the loss of red light under water is compensated for. The pre-processed images also look rather dull and faded which is the reason the camera manufacturers implement the enhancement functions.

### 4.2.3 Conclusions

We showed that for image colour restoration purposes there is a need to pre-process the images in order to remove or diminish the camera built in enhancement functions. The pre-processing step can be accomplished in an easy manner using a spectrometer, which measures the intensity values without any enhancement. It is enough to make data collection with the spectrometer once and then use the obtained coefficients for any imagery taken with that particular camera under similar conditions.

Based on the assumption that the camera's enhancement functions are linear, which we show in this work and Equation 4.10 we can use the ratio between the intensity counts of the spectrometer and the pixel intensities in the image to pre-process the entire image. The average values of red, green and blue are then serving as an input to the compensation enhancement function.

In this work we are assuming that the transmittance factor is negligible due to a very short distance between the object and the optic fiber. However, for the imagery made with the camera we could still evaluate the effects of water transmittance since the distance between the camera and the object is approximately 45 cm using a model for atmospheric correction. In this paper we did not perform tests on the field data.

We need to search for other methods that are easy to implement under the water. In this thesis we performed data collection and further correction and we could show that the small size of the spectrometer and a sufficient length of the fiber allow for spectral measurements under the water with little effort.

### 4.3 Paper V

#### Dissolved particles influence on $K_d$ values

The bluishness in images is caused by apparent optical properties of water where light in the red and yellow region of the spectra will be more attenuated with increasing depth than in the blue spectral region. [38]. However, not only the pure water itself will affect the optical climate of the water mass and affect the colour in the photos taken at different water depths, but also inherent optical properties will have impact. In waters it is possible to predict light attenuation by measuring or estimating  $K_d$  values. Strictly speaking,  $K_d$  is not a property of the water itself but rather a descriptor of the underwater light field that varies with depth, solar altitude, and time. In Paper V we show how to determine what  $K_d$  values should be used for colour restoration of imagery in three spectral channels. The process is automated and based on the absorption coefficients of dissolved organic matters.

So far our work has mainly been dealing with correction for the attenuation of the water itself. In a certain environment it could be recommendable to colour correct for or at least be aware of possible effects of substances in the water. Two essentially different types of substances or substance behaviour need to be discussed. We separate between dissolved and suspended matter. The dissolved matter is commonly of organic origin and usually named yellow substance. Also the salt in sea water could have some influence on the optical behaviour. The suspended matter could be either inorganic or organic and the organic matter could be dead or living. It is common to call the inorganic matter just suspended matter and it is also common to treat the phytoplankton separately, due to its water quality importance. Phytoplankton influence, however, is very complex and the complexity is much worse due to the fact that we always have a mixture of all three agents in natural waters.

In situ spectral absorption coefficient profiles can be measured with spectral radiometers [13]. In order to calculate the spectral absorption of a particular water layer it is enough to measure a spectra with a spectrometer. The instrument we use has 1 024 spectral channels and register pointwise the intensity counts. The concentration of dissolved organic matter is usually based on the amount of organic carbon present in the water. Experiments have shown that the spectral absorption of yellow substance varies approximately exponentially with wavelength and increases with decreasing wavelength [38]. Phytoplankton specific absorption coefficients have two absorption peaks at 440 and 675 nm. The peak at 440 nm is stronger than at 675 nm [1]. In clear near shore ocean waters the concentration of non-organic suspended matters is predominant, however we are not concerned with the calculation of those. Concentration of dissolved organic matters and chlorophyll may vary greatly for different diving sites and should thus be measured in situ or estimated from

measured irradiances.

### 4.3.1 Methods and experiments

As we have taken photographs in Florida, Portugal and Sweden we need to, at least theoretically, discuss the colour effects of substances in the water as suspended matter, phytoplankton and yellow substances are very common in those waters, typically a mixture of all three. In this paper we will discuss the combined effects of dissolved matter and phytoplankton.

#### **Absorption Coefficient for Dissolved Matters and Chlorophyll**

Concentration of dissolved organic matters in water can be expressed in terms of the absorption property of the matter. In phytoplankton-dominated waters near the sea surface, the total absorption and backscattering coefficients can be modelled as chlorophyll concentration  $C$  and yellow substance factor  $Y$  for each depth interval, see Equation 4.11 [1].

$$a(\lambda, z) = a_w(\lambda) + 0.06a_{ph}^*(\lambda)C(z)^{0.65} + Y(z)a_{ph}(440)\exp(-0.014(\lambda - 440)). \quad (4.11)$$

$Y$  describes the relationship between the absorption by yellow substance at 440 nm and the absorption by phytoplankton at 440 nm.

The equations 4.12 and 4.13 for concentration of chlorophyll and yellow substances below are from [1].

$$C = ((\delta_{ji}K_d - 0.686\delta_{st}K_d + 0.0753)/0.0746)^{1.54}, \quad (4.12)$$

$$Y = -(\delta_{ji}K_d + 0.0049 - 0.0107C^{0.65})/0.0625C^{0.65}, \quad (4.13)$$

where  $\delta_{ji}K_d = K_d(\lambda_j, zz_1) - K_d(\lambda_i, zz_1)$ . In this formula  $i$  and  $j$  denote different wavelengths. An analysis of the commonly used wavelengths in ocean colour measurements showed that the optimal wavelength pairs to solve these equations are (412, 443) and (443, 555) [1]. The  $a_w(\lambda)$  and  $a_{ph}^*$  coefficients are commonly used and found in [36, 30]. The  $K_d$  values that were used in the Equations above are estimated from intensity count measurements with a spectrometer at different depths. The absorption coefficients for the dissolved matters are plotted against the wavelengths and compared to the values of  $K_d$  for the respective wavelengths.

### 4.3.2 Results

By modelling the absorption behaviour for each available wavelength we can clearly see which wavelengths are more sensitive to the absorption of dissolved organic matters in the water. In Figures 4.8, 4.9 and 4.10 we see the  $K_d$  values and absorption coefficients, respectively, plotted as functions of wavelength. We set the values for  $K_d$ :s marked with  $\times$  in the colour reconstruction algorithm described in section 4.1.

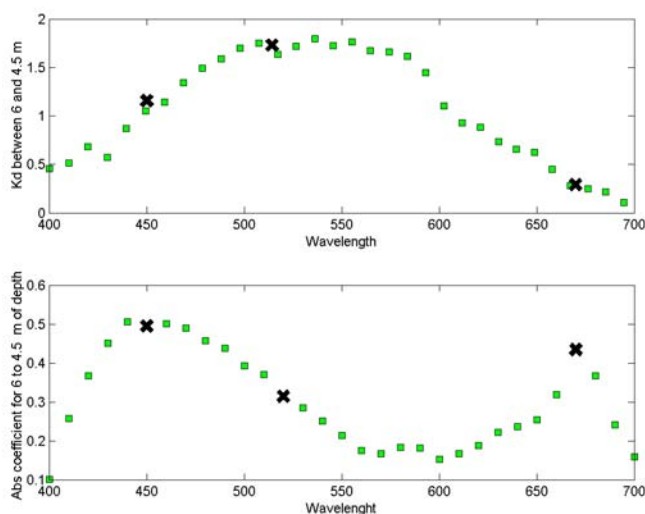


Figure 4.8:  $K_d$  used for correction of colours in images at depths between 6 m and 4.5 m compared to absorption coefficients.

The shape of the curves for the absorption coefficients shows the presence of phytoplankton in the water because of the two peaks at blue and red spectral intervals. When we colour correct the imagery with three spectral channels we use only three  $K_d$  values each, representing the red, green and blue spectral intervals. We can clearly see from Figures 4.8, 4.9 and 4.10 that  $K_d$  values representing the red spectral interval correspond to the same wavelength as the leftmost peak value of the absorption coefficient. The wavelength corresponding to the peak value of the absorption is the most attenuated and altered by the dissolved organic matters. Hence the new value for  $K_d$  should be taken from a wavelength that is not representative for the peak value of absorption to colour correct an image taken at this particular diving site. We test another value of  $K_d$  that is more appropriate and compare the two colour corrected images; one using the  $K_d$  values from the wavelength representing the top absorption of the dissolved matters and the other with the new  $K_d$ :s. Since there

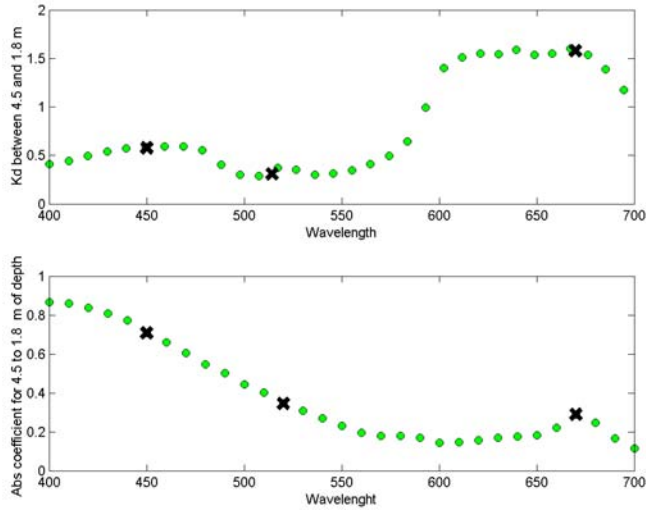


Figure 4.9:  $K_d$  used for correction of colours in images at depths between 4.5 m and 1.8 m compared to absorption coefficients.

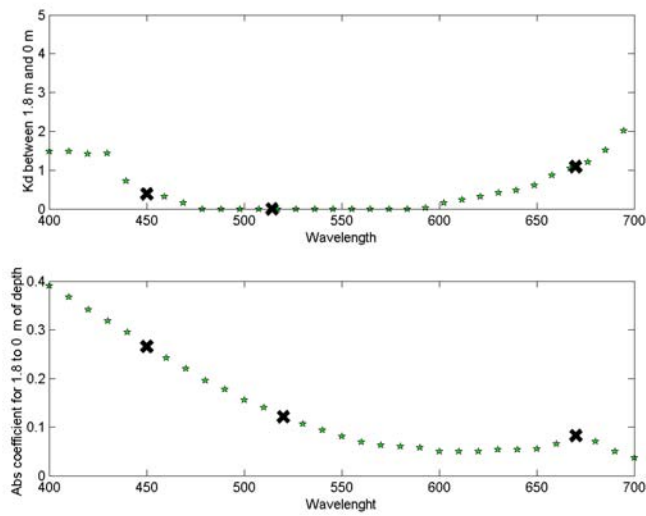


Figure 4.10:  $K_d$  used for correction of colours in images at depths between 1.8 m and 0 m compared to absorption coefficients.

is very little difference between the image's intensity values after colour correction and the effect therefore is hard to detect visually, we show in the Table

	Corrected with $K_d$ :s corresponding to the absorption peak	Corrected with new $K_d$ :s
Red	74	63
Green	36	32
Blue	35	31

Table 4.2: *Average intensity values of restored images.*

4.2 the average values for blue, green and red channels in the resulting images.

### 4.3.3 Conclusions

Underwater photographs used for the applications described in the Introduction are most commonly taken in coral reef environments and such waters are often very clear water with little material, suspended as well as dissolved. Typically, there are very low concentrations of small fractions of inorganic matter. Only occasionally a plankton bloom may occur. Our colour correction model is therefore often sufficient for photographing of reefs. However, in other types of open waters it could be of great importance to determine which water layers contain the most of dissolved organic matters. This knowledge would lead to a more careful choice of diffuse attenuation coefficients to be used in the colour correction algorithm.

For the imagery tested in this paper there was very little concentration of dissolved organic matters and therefore alternation of  $K_d$  values did not make a significant difference in the results. The choice of a new  $K_d$  value for the red, green and blue spectral intervals is user supervised, however we are looking for a method that will make this process automatic. The process of calculating  $K_d$  values automatically is discussed in Paper VI.



## 4.4 Paper VI, VII

### Spectral data applied on colour underwater image correction

Methods for careful monitoring, planning and management of marine environments have become essential [19]. So far we have discussed methods for colour correction of underwater images with three spectral channels.  $K_d$  values were obtained for three spectral channels and applied on each of the red, green and blue channels in the image. We came to realise that limitation in the amount of spectral channels leads to results that can only be validated for the digital camera that was used at the particular diving site. We need to establish better credibility of the methods described earlier in this thesis.

In this section we will introduce an expansion of the colour restoration concept brought up in previous sections. In Paper V the authors are arguing that the absorption coefficients of dissolved organic matters can give an indication about what  $K_d$  values should not be used in colour reconstruction of the images, but no discussion is given on which wavelengths that are appropriate to compute the  $K_d$  values needed in reconstruction of colours. In Paper VI we are addressing this issue by presenting a Stability Model which will give a value range for wavelengths used to compute  $K_d$  values that are as stable as possible in terms of variation with increasing depth.

Another aspect concerning the improvement of algorithm behaviour is the digital image itself. For our colour correction algorithm three spectral channels are somewhat insufficient. However, to keep the method as economically attractive as possible we need to hold on to the idea that digital images collected with off the shelf digital camera provides a sufficient information for colour restoration purposes. We believe that our method would benefit from using more spectral channels and we will show that spectral information obtained from the same scene as digital image will lay the foundations of creation of pseudo hyperspectral image.

We strive to improve the results obtained in previous sections significantly by expanding the imagery to more channels and colour correct each one of them. This process is discussed in Paper VII.

#### 4.4.1 Methods and experiments

We use spectral pointwise collected data and images with three spectral channels. In this study we rely on spectrometer measurements of a coloured plate and Spectralon at various depths. An image of the plate and the Spectralon was taken by a digital camera at the corresponding depth at the same time. The spectrometer's spectral data of each coloured plate gives a possibility to create pseudo hyperspectral imagery using a defined weighting function. Be-

fore building pseudo hyperspectral imagery we remove or at least significantly diminish the camera's built in enhancements effects. This process is addressed in Paper IV.

The large amount of obtained channels will give a more accurate representation of the imagery than that of classic red, green and blue. The imagery is then corrected using diffuse attenuation coefficients obtained from the spectra values.

As a result we show a RGB image, which is colour corrected by adding the light that has been attenuated. The difference between the results presented in previous sections and the results in this section is that we do operate with 1 024  $K_d$  values instead of only 3.

### Stability model to calculate the correct $K_d$ values, Paper VI

Data was collected off the coast of Gävle, Sweden, in May 2005. Solar altitude was  $42^\circ$ . For this study we used a spectrometer [27] and took measurements of a gray reflectance plate [21] under the water. We measured at depths between 0 m and 4 m with 20 cm intervals. The spectrometer registered pointwise the intensity counts in 1 024 spectral channels from 341.04 nm to 1019.74 nm with the wavelength resolution of 0.29 nm.

The intensity counts from a spectrometer are used here to obtain  $K_d$  values as a function of wavelength  $\lambda$  and the difference  $zz_1$  between two depths  $z$  and  $z_1$ , see Equation 4.14.

$$K_d(zz_1, \lambda) = \frac{I(\lambda, z_1) - I(\lambda, z)}{zz_1 I(\lambda, z)}, \quad (4.14)$$

where  $I(\lambda, z)$  is the intensity of wavelength  $\lambda$  at depth  $z$ .

The curves of  $K_d$  as a function of wavelength are jagged, due to particles in the water, reflection of solar light on waves and measurement errors, see Figure 4.11. Choosing wavelengths from the particularly jagged areas gives  $K_d$  values arbitrarily picked from a large interval. To minimise the arbitrariness, we calculate the subinterval where the curve is as smooth as possible.

The stability model for  $K_d$  values minimises the total rate of change in small subintervals, see Equation 4.15.

As a first step we divide the whole visible spectra in the red, green and blue intervals, respectively, according to the following: red: 630-700 nm, green: 500-570 nm and blue: 450-500 nm, [18]. Further we divide each of these intervals in small subintervals  $R_i, G_i$  and  $B_i$   $\lambda_1, \lambda_2, \dots, \lambda_n$ , where  $n = 22$  for  $R_i$ ,  $n = 21$  for  $R_g$  and  $n = 15$  for  $R_b$ .

As a second step we seek for each of red, green and blue, the subinterval  $R_i, G_i$  and  $B_i$  where

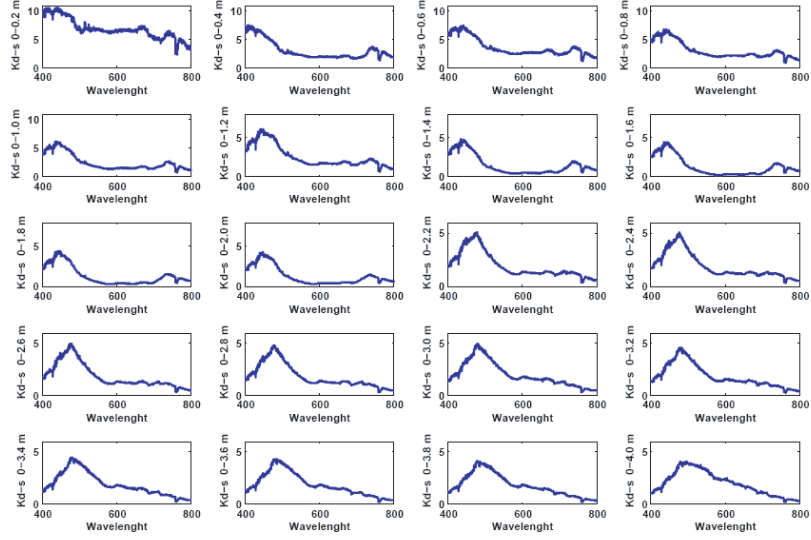


Figure 4.11: Curves of the  $K_d$  values as a function of wavelength for the depths from 0.2 to 4 m.

$$\sum_{\text{depth}} \sum_{i=1}^{n-1} |K_d(\lambda_i) - K_d(\lambda_{i+1})| \quad (4.15)$$

is minimal.

The subintervals in our case consists of ten different wavelengths 0.29 nm apart. For the subinterval where the expression in Equation 4.15 is minimal, we can use any of the ten wavelengths since they all correspond to roughly the same  $K_d$  value. This  $K_d$  value is then set into the colour correction algorithm, described earlier in this thesis.

#### 4.4.2 Results

The results are based on measurements collected in Swedish waters and the result of colour correction of underwater images from Portugal. We calculate new intensity values in the image taken at 6 meters of depth with the algorithm described in section 4.1. The new image will have a colour representation as if it was taken at 1.8 meters of depth.  $K_d$ s used for calculation of the new image are obtained using the stability model and for comparison we prepare the same operation with three user defined  $K_d$  values. Since it is difficult to visually decide from these images which  $K_d$ s gave the best result, we make a comparison with a reference image, which is actually taken with a digital camera at 1.8 m depth. The gray 99% reflectance plate is present on all im-

Channel	Image corrected with stability models $K_d$ -s	Image corrected with arbitrary $K_d$ -s
Red	6	14
Green	7	17
Blue	9	20

Table 4.3: *The absolute value of the difference with the reference image and the colour corrected images*

ages. We compare the average intensity of the gray plate on the image from 1.8 m depth, for red, green and blue channels with that of those two colour corrected images. In Table 4.3, the absolute values of the difference between the reference image and each of the colour corrected images are shown; one with the stability model's  $K_d$  values and one with the arbitrarily chosen  $K_d$  values.

#### 4.4.3 Conclusions

We have developed a stability model for obtaining suitable  $K_d$  values for colour reconstruction purposes automatically. As for the  $K_d$  values obtained from the imagery for three spectral channels, the data from which we establish these values should be collected once unless weather conditions change. The colour reconstruction method for underwater images described in this thesis is simple and economically defensible under condition that the correct  $K_d$  values are at disposal. Taking images under the water for scientific measurements differs from recreational underwater photography. With the possibility for colour correction marine scientists will not have to prepare the equipment necessary to create favourable light conditions. An analysis of the obtained  $K_d$  values suggests wavelength intervals, where  $K_d$  as a function of wavelength is optimally smooth, making these intervals suited for colour reconstruction purposes.

For the time being there are no digital hyperspectral cameras which would allow an extensive amount of  $K_d$  values to choose from, but we argue that the method is applicable to cameras with only three spectral channels. When spectral sensitivity curves for the camera are known it is easy to estimate the three  $K_d$  values representing wavelength range for red, green and blue channels.

For future work we would suggest an interpolation of spectral sensitivity curves built into the digital camera with the reflectance profile of the photographed object. This would give a much wider range of  $K_d$  values to be put into the stability model. Although the main *raison d'être* for the method is examining the health of corals, it is generally applicable to any type of water.

## Transformation to pseudo hyperspectral images from RGB imagery, Paper VII

The goal of Paper VII is to produce pseudo hyperspectral images from RGB images with the aid of the spectral point data. We have to use pointwise spectral data of red, green and blue patches at different depths. Furthermore, we have digital RGB images of the coloured patches and the surrounding environment at the same depths. Camera characteristics, see Figure 3.4, such as relative responses should ideally not affect the resulting hyperspectral image and are therefore corrected for.

Let  $Sp_r, Sp_g$  and  $Sp_b$  be vectors containing the spectral data from points with red, green and blue colour, respectively. E.g.  $Sp_r = [Sp(\lambda)]_{\lambda \in L}$ , where  $L$  is the set of wavelengths that spectral data has been collected for or some suitable subset.

Further, let  $0 \leq I_r, I_g, I_b \leq 255$  be the 95% percentile of the highest red, green and blue respectively intensity values from the corresponding channels in the image. When we divide the intensity values with the relative sensitivity  $RelS_r, RelS_g, RelS_b$  of the red, green and blue channels, respectively, in order to remove the characteristics of the camera, pseudo hyperspectral data representing the light present at the scene regardless of the sensitivity of either eye or camera for each pixel  $(x, y)$  is estimated as

$$Sp_f(x, y, \lambda) = \frac{f(x, y)}{I_f RelS_f(\lambda)} Sp_f(\lambda), f \in \{r, g, b\}, \quad (4.16)$$

where  $r(x, y), g(x, y)$  and  $b(x, y)$ , respectively, are the intensity values for red, green and blue at pixel  $(x, y)$ .

The result of this operation is a number of images equal to the number  $|L|$  of spectral channels in the spectrometer.

The rate at which light disappears with depth is calculated from spectral data given that exact depth measurements are made. The coefficients inserted into Beer's Law give us a prediction of how much light remains at a certain depth. The colour correction formula 4.17 is derived from Beer's Law.

$$I(z_1) = I(z) e^{K_d(z)z - K_d(z_1)z_1}, \quad (4.17)$$

where  $I(z)$  is the pixel intensity in the image for depth  $z$ .

We subject our hyperspectral data to this formula and as an outcome we will get the image as if it was taken at a much much more shallow depth than in reality. Colour correction is based on a specific value, not on aesthetical subjective supervision from the user.

All hyperspectral images will in this experiment be "lifted up" to a depth of 1.8 meters where almost all light is still present (i.e. have not been absorbed

by the water column). This statement applies only to the particular dive site where imagery was collected.

At this stage we have  $3|L|$  colour corrected images  $C_f^{\text{hyp}}(\lambda)$  for each of red, green and blue, representing one pseudo hyperspectral image. In order to produce a colour corrected RGB image from the pseudo hyperspectral image we build the red channel by weighing the “red” images  $Sp_r(x, y, \lambda)$  according to the camera’s relative response  $RelS_r(\lambda)$ , and correspondingly for the green and blue channels, see Equation 4.18.

$$C_f^{\text{RGB}}(x, y) = \frac{\sum_{\lambda \in L} C_f^{\text{hyp}}(x, y, \lambda) RelS_f(\lambda)}{\sum_{\lambda \in L} RelS_f(\lambda)}, f \in \{r, g, b\}. \quad (4.18)$$

Remember that we divided the intensity values of the pseudo hyperspectral images with the camera’s relative sensitivities, so to get an RGB image that makes sense visually we need to multiply with the relative sensitivities. In this way we also produce the resulting RGB image as a weighted average of the pseudo hyperspectral images in a natural way, since the relative sensitivity can be seen as a measure of how representative a certain wavelength is for a spectral channel.

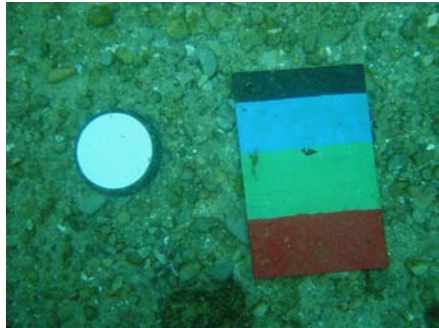
#### 4.4.4 Results

We have showed a method of transforming an RGB image into pseudo hyperspectral data. The data is then colour corrected in each spectral channel and brought back into the original representation of only three spectral channels. To illustrate the proposed method we compare the result archived in hyperspectral imagery with the colour correction performed on three channels R, G and B, see Figure 4.12.

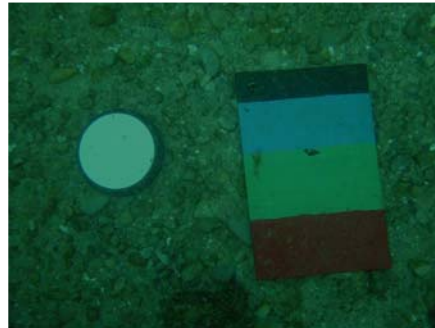
We have shown that a multispectral image with only three channels can be transformed into pseudo hyperspectral imagery with little computational effort.

When a hyperspectral image is transformed back into three channel form, the weighting function will pick the most representative channel in the red, green and blue spectral interval based on the sensitivity curves of the camera.

The coloured plate shown in the image regained its colours as if lighting conditions corresponded to those at 1.8 m of depth. We compared the pixel values of 95% percentile for the red, green and blue channels of the corrected image to the pixels of the image that was actually taken at 1.8 m. The difference for each of the three channels; red, green and blue, is less than 9 in intensities.



(a) Original image taken at 6 m of depth.



(b) Pre-processed with enhancement coefficients to remove the cameras beautifying functions.



(c) Colour corrected by applying the  $K_d$ 's at each of the three channels, which have an effect of bringing up the image to 1.8 m of depth.



(d) Colour corrected (in effect bringing the image up to 1.8 m) pseudo hyperspectral images and transformed back to RGB model.

*Figure 4.12:* Underwater image colour corrected by bringing it up to 1.8 m depth.

#### 4.4.5 Conclusions

As we can see in Figure 4.12 (c), the outcome of the colour correction algorithm performed on only three spectral channels for this particular image is erroneous. The resulting image is almost black. In contrast, colour correction done on pseudo hyperspectral data derived from this image is highly successful. This leads us to the conclusion that for colour correction purposes of underwater images it is beneficial to use more than three spectral channels.

The method can produce pseudo hyperspectral images with as many different channels as the spectrometer can capture, but in this Paper, experiments are performed using only 21 different wavelengths (7 for the red, green and blue spectral intervals respectively) with good result. The limitation of the number of channels is due to Matlab's computational time and memory overload.

Paper VII suggests that pseudo multispectral or hyperspectral images may

be acquired with a simple photometer and a few filters instead of a spectrometer, making the process even more economically defensible. So far, there are no known simple methods to acquire instantaneous hyperspectral imagery using multiple filters under the water.



## 5. Discussion

In this thesis we tested and developed methods for colour correction of underwater images. We chose to confine our interest to simple and inexpensive methods. In the present methodology for colour restoration of underwater imagery there is no clear indication of how to use the optical properties of water to obtain the correct intensity values of the image. In this work we showed that it is possible to incorporate knowledge about absorption, reflection and transmission of light in the water into a colour correction model.

During the work on this thesis the method went through modifications and improvements. The basic idea is to use Beer's Law and put parameters such as attenuation coefficients and depth into it. The estimation of these parameters from underwater images and tests are described in Papers I and II. Considering the camera built in enhancement functions makes an improvement for the method and this issue is addressed in Papers III and IV. Finally, we further advance the method by introducing the Stability model for  $K_d$  values and split an RGB underwater image into pseudo hyperspectral image where each channel undergoes the colour correction by the basic method.

There are advantages and disadvantages with the chosen method for colour correction. It is clear that for the images used in this thesis the method works satisfactory, however, we do not know other than in theory whether the method could be generally applied since we have a limited set of images available. Also, processing a great number of images would be computationally demanding. Furthermore, the properties of underwater environments are diverse, not only over different locations, but also over time. Another problem is that  $K_d$  values do not always follow an exponential rate due to different layers in the water. In Paper V we show how to distinguish these different layers. As a future work in this area of research we suggest an incorporation of the effect of different layers in the water into the colour correction algorithm.

The advantages of our method is that it is cost effective and easy to implement. The method can be used as a complement to e.g. monitoring the health of coral reefs from space, which is the currently most used method. For our model the crucial parameters are the diffuse attenuation coefficients, which we estimate from images or spectral pointwise measurements. These values can be accessed from the mooring stations, which are placed in different oceans sometimes very close to shore. Unfortunately, there are only a few such sta-

tions as of now; a greater proliferation of these would make colour correction according to our model even more practical and exact.

There are no cameras that can collect instantaneous hyperspectral images. Such images would be possible to create by using spectrometers that allow for linewise detection, but this would require a very precise positioning of the instrument and be very time consuming. Under water, precise positioning is nearly impossible since the stability of the instrument would be disturbed by currents and other water movements. Besides, when taking data under the water, we are always limited in time.

In this thesis we show a method that makes it possible to create pseudo hyperspectral images without leaving a computer lab, provided that there are available pointwise spectral data from the same scene as the RGB image. It would be possible to collect the necessary data with a photometer and a collection of filters instead of a spectrometer. At present, this would be hard to do in practice, but it is an interesting future work to investigate the development of a viable method for acquisition of data with a photometer.

The suggested colour correction method is based on a few transparent and simple ideas; therefore it is easy to see that it is theoretically sound. Also, the performed experiments confirm the correctness of the algorithm.

## Sammanfattning

Forskningsuppgiften inriktar sig på analys och färgkorrigering av undervattensbilder. Undervattensbilder används som kompletteringsdata för olika studier av marina miljöer. Den här avhandlingen syftar främst på applikationer inom öppna vattnen med korallrev. Koraller producerar mer syre än all kvarvarande regnskog i världen. Miljoner människor lever på fiske som bedrivs nära korallreven och risken finns att med korallrevens försvinnande runt om i världen kommer dessa människor att förlora källan till välstånd. Vatten täcker ca 70% av jordens yta och är världens minst utforskade område. Begränsningen ligger i att människan inte kan befinna sig under vatten hur länge som helst. Dyra och ofta otympliga instrument och apparater måste användas för att samla information om undervattensmiljön. Detta leder till stora svårigheter för forskning på vattenlevande organismer och andra undervattensobjekt.

I den här avhandlingen diskuteras metoder för att ta digitala bilder med en billig och enkel utrustning på undervattensobjekt och studera bilderna med hjälp av dator. Eftersom vatten absorberar ljus mycket mer än luft måste nya metoder utvecklas som kan korrigera färger i de tagna bilderna. De flesta bilder som tas under vattnet kommer att ha dominerande blå färg. Detta är på grund av att det blåa ljuset absorberas "långsammare" än andra färger. Det är viktigt att skilja på korrigering och förbättring av färger i bilder. Med korrigering menas återställandet av riktiga färger, som de förekommer i verkligheten. Förbättring av färgerna är en subjektiv process som baseras på varje människas estetiska upplevelse.

Metoderna grundar sig på uppskattning av den "hastighet" med vilken varje ljus (rött, grönt och blått) försvinner med djupet. Därefter kan man addera det försvunna ljuset till bilden och därmed få den att se ut som om bilden är tagen vid ytan. Det är mycket viktigt för färgkorrigeringsalgoritmen att tillhandahålla korrekta värden för hur "snabbt" ljuset försvinner med djupet. De värdena kallas *attenueringskoefficienterna* och betecknas i avhandlingen som  $K_d$  värdena.

En spektrometer används i det här arbetet. Med det instrumentet kan man mäta den verkliga ljusintensiteten för olika våglängder och jämföra dem med kamerans utdata. Detta har gett underlag för en bättre uppskattning av det degraderade ljuset och har dessutom använts som referensdata för att kalibrera

digitala kameror. En metod för att uppskatta förbättringsfunktionerna, som alltid byggs in i de billigare digitala kamerorna, har tagits fram. Baserad på slutsatserna dragna i artikel IV kan man föreslå att alla digitala bilder tagna för forskningssyfte bör förbehandlas med koefficienter som minskar effekten av förbättringsfunktionerna inne i kameran.

Vi har konstaterat att tre spektrala kanaler inte alltid är tillräckligt för färgkorrigeringssyften. Ljuset av lägre energier försvinner "först" när det passerar vatten. Detta leder till att vi får väldigt lite användbar information från den röda kanalen i digitala bilder. Därför söker vi efter metoder som ger oss möjlighet att arbeta med flera spektrala kanaler utan att behöva använda dyrbar utrustning. Spektrometern har använts i det här avhandlingsarbetet för att utveckla en metod för att skapa pseudohyperspektrala data från bilder som innehåller tre spektrala kanaler: röd, grön och blå. Den metoden beskrivs i artikel VII. Det uppskattade hyperspektrala data har korrigerats med metoden som beskrivs i artiklarna I och II. Resultaten visar att man med enkel utrustning och med en dator kan utföra automatisk färgkorrigering av undervattensbilder. Den erhållna färgåtergivningen som bättre avspeglar verkligheten bör vara värdefull för forskare som iakttar ändringar i korallreven, skapar bottenkartor eller utför arkeologiska arbeten under vatten.

## Acknowledgments

The work leading to this thesis has been supported by my friends and colleagues at the Centre for Image Analysis (CBA) and University of Gävle. My family has provided a continuous encouragement. I would like to thank the following people in particular:

- Ewert Bengtsson, my supervisor, for being accessible and offering me help and guidance, for being understanding and letting me work independently with the things that interested me the most, and for making sure that I stay on the right track.
- Knowledge Foundation, for financing my PhD studies.
- Ass. Prof. Tommy Lindell for his ability to distinguish important from unimportant when proofreading my articles and discussing the ongoing work.
- Gunilla Borgefors, Ingela Nyström, Petra Philipsson, Carolina Wälby, Bosse Nordin for making the environment at CBA very welcoming.
- Lena Wadelius, for answering all complicated administrative questions for me and being very professional in task management.
- All my proofreaders; David and Marta, for correcting my English and mathematical expressions.
- ♡ David Sundgren, for being there for me twenty-four hours.
- ♡ Marta Siborelius for never doubting.
- ♡ Christer, for useful advices on data collection and for putting up with me during this period.
- ♡ Irina, for your ability to make me see things from a totally different angle. You are the best!

Thank you!

Julia  
Gävle, September 2005



## References

- [1] S. Abbott M. R. Letelier R. M. Bartlett, J. and G. Richman, J. Chlorophyll concentration estimated from irradiance measurements at fluctuating depths. In *Proc. The Ocean Optics Conference*, 1998.
- [2] Burke L. McManus J. Spalding M. Bryant, D. Reefs at risk: a map-based indication of threats to the world's coral reefs. In *World Resources Institute*, page 56, 1998.
- [3] P. W. Daly C., Fröhlich. Data on total and spectral solar irradiance: comments. *Appl. Opt.*, 22, 3928, 1983.
- [4] M. Caimi, F. Selected papers on underwater optics. *International Society for Optical Engineering Milestone Series*, 118, 1995.
- [5] J. Convell. Underwater correction. WWW document, October 2003. <http://share.studio.adobe.com/axAssetDetailSubmit.asp?aID=8419&sar=1>.
- [6] D. Davis. *Adventures in Physics*. McGraw-Hill Companies, 1st edition, 1999.
- [7] R. Delfs. Getting rid of the underwater blues. WWW document, February 2005. <http://www.wetpixel.com>.
- [8] L. Estep. Backscatter of bottom reflected light into the downwelling light stream. *Office of Scientific and Technical Information, OSTI*, 1992.
- [9] Y. Fissenko V. T. Rogatchev G. A. Fissenko, T. and A. Sushechev. G. An interpolation method for color image reconstruction in deep underwater observation. In *Proc. of D. S. Rozhdestvensky Optical Society: The II International Conference, Current Problems in Optics of Natural Waters*, pages 113–118, 2003.
- [10] Clark C. Mumby P. Edwards A. Ellis A. Green, E. Remote sensing techniques for mangrove mapping. *Journal of Remote Sensing*, 19(5):935–956, 1998.
- [11] T. Grey. *Color Confidence: The Digital Photographer's Guide to Color Management*. Sybex, 1st edition, 2004.

- [12] Hamid Mohammed H. and F. Bergholm. Sensitivity analysis of multi-channel images intended for spectrometry applications. *Submitted for publication*, 2005.
- [13] K. Hojerslev, N. A spectral light absorption meter for measurements in the sea. *Limnology, Oceanography*, 20(5):1024–1034, 1975.
- [14] LeDrew E. Holden, H. Effects of the water column on hyperspectral reflectance of submerged coral reef features. *Bulletin of Marine Science*, 2000.
- [15] Gerald C. Holst. *CCD Arrays, Cameras, and Displays*. SPIE-International Society for Optical Engine, 2nd edition, 1998.
- [16] R.W.G. Hunt. *Measuring Colour*. Fountain Press, England, 3rd edition, 1998.
- [17] Dera J. Underwater irradiance as a factor affecting primary production. In *IO PAS*, 1995.
- [18] Childers R. Jones, E. *Contemporary College Physics*. John Wiley & Sons, Inc, 2nd edition, 1999.
- [19] LeDrew E. Holden H. Knight, D. Mapping submerged corals in fiji from remote sensing and in situ measurements: applications for integrated coastal zone management. *Oceans and Coastal Management*, 34(2):153–170, 1997.
- [20] Kohler D. Kohler, A. *Underwater Photography Handbook*. New Holland Publishers, 1st edition, 1998.
- [21] Labsphere. Spectralon : Reflectance material for component fabrication. WWW document, November 2002. <http://www.labsphere.com/products.asp>.
- [22] Carder K. L. Chen R. F. Lee, Z. and G. Peacock, T. Properties of the water column and bottom derived from airborne visible infrared imaging spectrometer (aviris) data. *Journal of Geophysical Research*, Vol. 106, No. C6, pages 11639–11651, 2001.
- [23] P. Carder K. L. Steward R. G. Lee, Z. and G. Peacock, T. An empirical algorithm for light absorption by ocean water based on color. *Journal of Geophysical Research*, 103:27967–27978, November 1998.
- [24] Chang W.C. Liew S.C. Lim, A. and L.K. Kwoh. Computation of atmospheric water vapour map from modis data for cloud-free pixels. In *Proc. The 23rd Asian Conference on Remote Sensing*, 2002.
- [25] V. Hvalac M., Sonka and Boyle R. *Image Processing, Analysis, and Machine Vision*. Thomson Publishing, 2nd edition, 2000.



- [26] Curtis D. Mobley. *Light and Water Radiative Transfer in Natural Waters*. Office of Naval Research, 2nd edition, 2004.
- [27] Ocean Optics. Usb spectrometer. WWW document, August 2004. <http://www.oceanoptics.org/products/usb2000.asp>.
- [28] K. Miyata P. Stigell and M. Hauta-Kasari. Wiener estimation method in estimation of spectral reflectance from rgb images. In *Proc. of the 7th International Conference on Pattern Recognition and Image Analysis (PRIA-7-2004)*, pages 398–401, 2004.
- [29] A. Popov, S. and M. Emelyanov, G. Color correction of digital images. *Pattern Recognition and Image Analysis*, 13(4):678–681, April 2003.
- [30] L. Prieur and Sathyendranath. An optical classification of coastal and oceanic waters based on the specific spectral absorption curves of phytoplankton pigments dissolved organic matter and other particulate materials for 400-700 nm. *Limnology Oceanography*, 26(4):671–689, 1981.
- [31] C. Quirolo. Reef relief a non-profit grassroots membership organization dedicated to preserve and protect living coral reef ecosystems through local, regional and international efforts. WWW document, August 2004. <http://www.reefrelief.org/>.
- [32] Gonzales R. and Woods R. *Digital Image Processing*. 2nd edition, 2003.
- [33] Smith R., C. and Baker K. The bio-optical state of ocean waters and remote sensing. *Limnology Oceanography*, 23(2):247, 1978.
- [34] J. Sangwine, S. and A. Ell, T. Colour image filters based on hypercomplex convolution. *VISP*, 147(2):89, April 2000.
- [35] J. Sangwine, S. and A. Ell, T. Hypercomplex fourier transforms of color images. In *ICIP01*, pages 137–140, 2001.
- [36] C. Smith, R. and K. S. Baker. Optical properties of the clearest natural waters (200-800) nm. *Appl. Opt*, 20(4):177–184, 1981.
- [37] W. Fontes N. R. Therrien, C. *Performance Analysis of the Wiener Filter with Applications to Underwater Acoustic Signals*. Storming Media, 1st edition, 1997.
- [38] R.E. Walker. *Marine Light Field Statistics*. John Wiley & Sons, Inc, 1st edition, 1994.
- [39] Woods Hole Oceanographic Institution (WHOI). Upper ocean mooring data archive. WWW document, October 2005. [http://www.whoi.edu/home/research/data\\_center.html](http://www.whoi.edu/home/research/data_center.html).

# Acta Universitatis Upsaliensis

*Digital Comprehensive Summaries of Uppsala Dissertations  
from the Faculty of Science and Technology 120*

Editor: The Dean of the Faculty of Science and Technology

A doctoral dissertation from the Faculty of Science and Technology, Uppsala University, is usually a summary of a number of papers. A few copies of the complete dissertation are kept at major Swedish research libraries, while the summary alone is distributed internationally through the series Digital Comprehensive Summaries of Uppsala Dissertations from the Faculty of Science and Technology. (Prior to January, 2005, the series was published under the title "Comprehensive Summaries of Uppsala Dissertations from the Faculty of Science and Technology".)

Distribution: [publications.uu.se](http://publications.uu.se)  
urn:nbn:se:uu:diva-6138



ACTA  
UNIVERSITATIS  
UPSALIENSIS  
UPPSALA  
2005